Journal of Medicinal Chemistry

Article

pubs.acs.org/jmc

Converting Potent Indeno[1,2-*b*]indole Inhibitors of Protein Kinase CK2 into Selective Inhibitors of the Breast Cancer Resistance Protein ABCG2

Gustavo Jabor Gozzi,[†,‡,×] Zouhair Bouaziz,[§,×] Evelyn Winter,[†,∥] Nathalia Daflon-Yunes,[†] Dagmar Aichele,[⊥] Abdelhamid Nacereddine,[§] Christelle Marminon,[§] Glaucio Valdameri,[†,‡] Waël Zeinyeh,[§] Andre Bollacke,[⊥] Jean Guillon,[#] Aline Lacoudre,[∞] Noël Pinaud,[∞] Silvia M. Cadena,[‡] Joachim Jose,[⊥] Marc Le Borgne,[§,○] and Attilio Di Pietro*[,†,○]

[†]Equipe Labellisée Ligue 2014, BMSSI UMR 5086 CNRS/Université Lyon 1, IBCP, 69367 Lyon, France

[‡]Department of Biochemistry and Molecular Biology, Federal University of Paraná, Curitiba, Paraná 80060-000, Brazil

[§]Université de Lyon, Université Lyon 1, Faculté de Pharmacie, ISPB, EA 4446 Biomolécules Cancer et Chimiorésistances, SFR Santé Lyon-Est CNRS UMS3453-INSERM US7, 8 Avenue Rockefeller, F-69373 Lyon Cedex 8, France

[∥]Department of Pharmaceutical Sciences, PGFAR, Federal University of Santa Catarina, Florianopolis, Santa Catarina 88040-900, Brazil

[⊥]Institute of Pharmaceutical and Medicinal Chemistry, PharmaCampus, Westfälische Wilhelms-University Münster, Corrensstrasse 48, 48149 Münster, Germany

[#]Université de Bordeaux, UFR des Sciences Pharmaceutiques, INSERM U869, Laboratoire ARNA, 146 Rue Léo Saignat, F-33076 Bordeaux Cedex, France

[∞]ISM-CNRS UMR 5255, Université de Bordeaux, 351 Cours de la Libération, F-33405 Talence Cedex, France

ABSTRACT: A series of indeno[1,2-*b*]indole-9,10-dione derivatives were synthesized as human casein kinase II (CK2) inhibitors. The most potent inhibitors contained a N^5-isopropyl substituent on the C-ring. The same series of compounds was found to also inhibit the breast cancer resistance protein ABCG2 but with totally different structure−activity relationships: a N^5-phenethyl substituent was critical, and additional hydrophobic substituents at position 7 or 8 of the D-ring or a methoxy at phenethyl position ortho or meta also contributed to inhibition. The best ABCG2 inhibitors, such as **4c**, **4h**, **4i**, **4j**, and **4k**, behaved as very weak inhibitors of CK2, whereas the most potent CK2 inhibitors, such as **4a**, **4p**, and **4e**, displayed limited interaction with ABCG2. It was therefore possible to convert, through suitable substitutions of the indeno[1,2-*b*]indole-9,10-dione scaffold, potent CK2 inhibitors into selective ABCG2 inhibitors and vice versa. In addition, some of the best ABCG2 inhibitors, which displayed a very low cytotoxicity, thus giving a high therapeutic ratio, and appeared not to be transported, constitute promising candidates for further investigations.

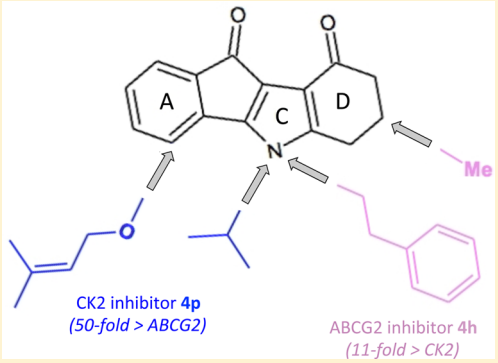

INTRODUCTION

Human protein kinase casein kinase II (CK2) is a highly pleiotropic serine/threonine protein kinase discovered in 1954.[1] Overexpression of CK2 and its elevated activity are closely related to many human cancers, including breast,[2] lung,[3] pancreas,[4] and prostate.[5] Recent studies also confirmed CK2 as a key target in leukemia[6] and glioblastoma.[7] One of the most remarkable features of CK2 is the existence of several forms: (i) catalytic CK2α subunit and its isoforms CK2α' and CK2α'', (ii) regulatory CK2β subunit, and (iii) heterotetramer composed of two catalytic subunits and two regulatory subunits.[8] Both CK2 heterotetrameric holoenzyme and its isolated catalytic subunits are constitutively active. Recent structural insights of CK2α, CK2β, and CK2 (quaternary structure of CK2) gave further knowledge to perform tailor-made compounds.[9−11] Thus, CK2 is becoming an important drug target for the 21st century as mentioned by E. G. Krebs in 1999.[12] Intensive drug discovery chemistry is currently leading to design and synthesis of small molecule CK2 inhibitors targeting ATP-binding pocket or exosites at the CK2α/ CK2β interface.[13] For example, we developed diverse indeno[1,2-*b*]indole- and pyrrolo[1,2-*a*]-quinoxaline-based scaffolds[14,15] as ATP-competitive inhibitors of CK2. Tetracyclic indeno[1,2-*b*]indole derivatives offer great opportunities to functionalize A-, C-, and D-rings and so access

Special Issue: New Frontiers in Kinases

Received: June 20, 2014
Published: October 1, 2014

   dx.doi.org/10.1021/jm500943z | *J. Med. Chem.* 2015, 58, 265−277

inhibitors with submicromolar IC_{50} and antiproliferative activity against cancer cell lines.[16]

Protein kinase inhibitors were previously shown to interact with multidrug ABC transporters involved in cancer cells resistance to chemotherapy. Protein kinase C inhibitors were able to inhibit P-glycoprotein/ABCB1 and homologues from yeast and protozoan parasites.[17] A number of tyrosine kinase inhibitors were found to strongly inhibit the breast cancer resistance protein ABCG2: canertinib (CI1033),[18] imatinib,[19] gefitinib,[20] *N*-[4-[(3-bromophenyl)amino]-6-quinazolinyl]-2-butynamide (EKI-785),[21] nilotinib and dasatinib,[22] vandetinib, pelitinib, and neratinib,[23] erlotinib,[24] sorafenib,[25] sunitinib,[26] and linsitinib.[27] Bisindolylmaleimides and indolocarbazoles[28] as well as dimethoxyaurones,[29] which inhibit various serine/threonine kinases, were also found to inhibit ABCG2.

ABCG2 is overexpressed in many types of tumors[30] and is recognized to play a role in their multidrug resistance by catalyzing the efflux of anticancer drugs. Potent, selective, and nontoxic inhibitors might constitute a good therapeutic strategy to improve anticancer drugs efficiency by increasing their bioavailability and then sensitizing tumor growth to their cytotoxicity.[31,32] New inhibitors should therefore be investigated. Our aim was to check the capacity of the newly synthesized indenoindole inhibitors of CK2 to interact with ABCG2 and inhibit its drug-efflux activity. It is shown that they indeed inhibit ABCG2-mediated mitoxantrone transport but importantly the structure−activity relationships are totally different from those governing CK2 inhibition.

CHEMISTRY

Tetrahydroindeno[1,2-*b*]indole-9,10-diones **4** were synthesized according to a previously reported method,[14,33] with a modification of the reagent for the deoxygenation of the *vic*-dihydroxyindeno[1,2-*b*]indole-9,10-diones **3**. Usually transition from **3** to **4** is performed with tetramethylthionylamide (TMTA); nevertheless we observed better yields with the tetraethylthionylamide (TETA).[34] The latter was prepared by slow addition of thionyl chloride to 4 equiv of diethylamine in dry ether at −40 °C.

The synthetic route started with the preparation of the corresponding enaminones **2**, readily available in very good yields by reacting substituted cyclohexane-1,3-diones **1** with primary amines. Subsequent condensation of **2** with 2,2-dihydroxyindane-1,3-diones (ninhydrins) afforded dihydroxyindeno[1,2-*b*]indole-9,10-diones **3** (Scheme 1).

Scheme 1[a]

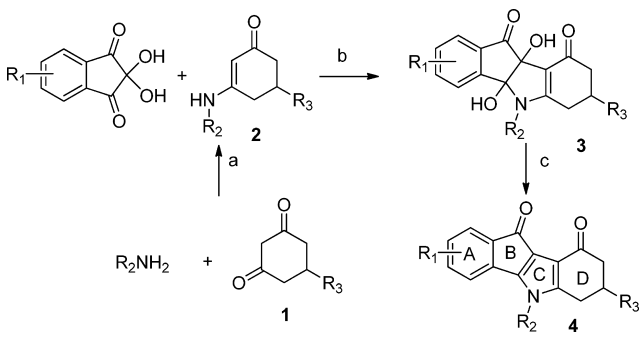

[a]Reagents and conditions: (a) toluene, reflux; (b) MeOH, rt; (c) $(NEt_2)_2SO$ (TETA), DMF, AcOH, rt.

This protocol provided a useful way to modify the substituents R_1, R_2, and R_3 in order to establish structure−activity relationships (CK2 inhibition, ABCG2 inhibition, and cytotoxicity). Structural variations on the A-, C-, and/or D-ring of the indeno[1,2-*b*]indole scaffold have been carried out using ninhydrins, primary amines, and cyclohexane-1,3-diones, respectively.

The 1- and 4-hydroxylated indenoindoles **4m** and **4n** (Scheme 2) were prepared from enaminone **2a** and 4-hydroxyninhydrin. The latter was readily prepared in two steps. First, the commercially available dihydrocoumarin reacted with $AlCl_3$ to afford the 4-hydroxyindan-1-one[35] which was then oxidized with SeO_2 in dioxane under microwave irradiation (unpublished data).

Condensation of 4-hydroxyninhydrin with enaminon **2a** led to the trihydroxylated derivatives **3m** and **3n** as a mixture of two regioisomers (ratio **3m**/**3n**, 78/22) which could not be separated under the classical conditions. Deoxygenation procedure of the mixture using TETA was carried out to afford the corresponding hydroxyindenoindoles **4m** and **4n**. At this step, the two regioisomers were easily separated by chromatography column and identified by NMR.

O-Prenylation of the 4-hydroxy derivative **4n** was performed with prenyl bromide in the presence of K_2CO_3 in acetone at reflux to provide derivative **4p** with 60% yield. The reaction with the isomer **4m** was more difficult, probably because of a hydrogen bond between the H of the phenol on the C-1 and the O of ketone C-10 that forms a pseudo six-membered ring more stable, so more difficult to break. Therefore, O-prenylation of the 1-hydroxy derivative **4m** was carried out by means of K_2CO_3 in dimethylacetamide (DMA) at 80 °C to provide derivative **4o** with 27% yield.

Assignment of regiochemistry was established for each regioisomer by NOESY. Compounds **4q** and **4r** were obtained by alkylation of 5,6,7,8-tetrahydroindeno[1,2-*b*]indole-9,10-dione **4a** with CH_3I and $PhCH_2Br$, respectively, in the presence of a solution of lithium cyclohexylisopropylamide (LCIA)[36] prepared from cyclohexylisopropylamine and *n*-BuLi in dry THF at −40 °C (Scheme 3). Attempts to improve the yield of these alkylations by modification of the reaction conditions (nature and amount of the base, amount of the alkylating agent, temperature) proved to be unsuccessful. Moreover, methylation provided the monomethylated compound **4q** with 10% yield and only traces of the dimethylated derivative when benzylation afforded only the disubstituted compound **4r** with 35% yield; the monobenzylated product was not detected. In either case, a large amount of degradation products was observed.

Altogether, 18 indeno[1,2-*b*]indole-9,10-dione derivatives have been synthesized, and their different substituents are shown in Figure 1.

The 3D structure of **4c** was determined by X-ray crystallography (Figure 2) and confirmed that expected on the basis of IR and ^1H NMR data. The key bond lengths and angles of this indeno[1,2-*b*]indole-9,10-dione **4c** are very similar to those given in the literature for other substituted indenoindole derivatives.[38,39] The 7,8-dihydro-6*H*-indeno[1,2-*b*]indole-9,10-dione system of **4c** is not planar; a derivation of the C12 and C13 atoms was noticed at 0.1935(3) and 0.4429(3) Å, respectively, from the plane defined by the heterotetracyclic system. The nonplanarity of this tetracyclic sytem is an important structural characteristic in contrast to planar polycyclic aromatic compounds. The double bonds C1═O1 and C11═O2 of the heterocyclic system of **4c** are

dx.doi.org/10.1021/jm500943z | J. Med. Chem. 2015, 58, 265−277

Scheme 2[a]

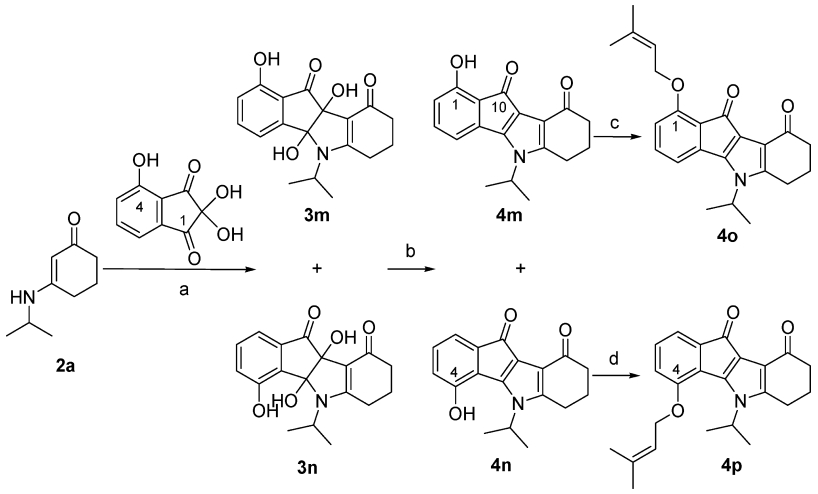

[a]Reagents and conditions: (a) MeOH, rt; (b) $(NEt_2)_2SO$ (TETA), DMF, AcOH, rt; (c) K_2CO_3, DMA, 80 °C, 24 h; (d) K_2CO_3, acetone, reflux, 8 h.

Scheme 3[a]

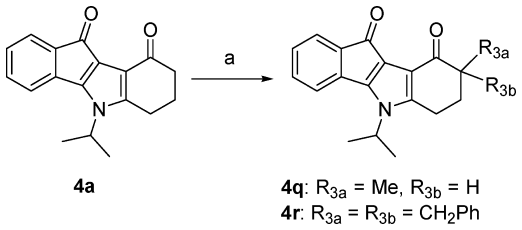

[a]Reagents and conditions: (a) cyclohexylisopropylamine, *n*-BuLi, THF, CH_3I or $PhCH_2Br$, −40 °C.

confirmed by their respective lengths of 1.218(3) and 1.221(3) Å.

BIOLOGICAL EVALUATION, SARS, AND DISCUSSION

The synthesized indeno[1,2-*b*]indoles were screened for their inhibition capacity, first against protein kinase CK2 and then against ABCG2, as summarized here below.

Inhibition of Human CK2 Holoenzyme. Comparison of the results in Table 1 allowed us to draw the following structure−activity relationships: (i) compound **4a**, with a N^5-isopropyl-substituted C-ring, produced a complete inhibition at 10 μM, with a good potency (IC_{50} = 0.36 μM); (ii) a 14-fold increased potency was observed with **4p** substituted at position 4 of A-ring with *O*-3,3-dimethylallyl ("prenyl"), which was higher than most of the reference inhibitors and approached the extremely potent silmitasertib (CX-4945[40]); by contrast, the same prenyl substituent at position 1 in **4o** dramatically altered the inhibition capacity to 44% at 10 μM; (iii) a 2-fold increased potency was produced by a methyl substituent at position 7 of D-ring in **4e** (IC_{50} = 0.17 μM), whereas a strong negative effect was observed at vicinal position 8 with either the same substitution in **4q** or a very hydrophobic and steric substitution by two benzyl groups in **4r** ($IC_{50} \geq 9.2$ μM); (iv) replacing the N^5-isopropyl by a benzyl in **4b**, a phenethyl in **4c**, or a phenpropyl in **4d** produced a marked alteration of inhibition (≥17-fold) by comparison to **4a**; a partial recovery in potency was produced when substituting with a methoxy the phenethyl at position ortho in **4j**, by 5.6-fold relative to **4c**, while the effects were lower at either position para in **4l** or meta in **4k**; (v) finally, a negative contribution of phenyl substitution at position 7 was observed when comparing **4g** to **4b**, and **4i** to **4c**. The concentration dependence of the inhibition of CK2 activity is illustrated in Figure 3 for the three best indenoindole inhibitors and the most potent reference inhibitor.

Inhibition of MCF-7 Cell Proliferation by the CK2 Inhibitor 4p. The antiproliferative effect of prenyl-substituted indeno[1,2-*b*]indole **4p**, which appeared to be the most potent CK2 inhibitor with an IC_{50} value of 25 nM, was evaluated in MCF-7 breast cancer cells.[41] For this purpose, a commercially available EdU-click assay was applied, resulting in the incorporation of a TAMRA fluorophore into the nucleic acid of cells performing DNA replication and preparing cell proliferation.[42] Proliferating cells can be recognized by a violet fluorescence of their nuclei (Figure 4B), and the number of such cells are counted with and without inhibitor and set into relation of the corresponding number of control cells.

As shown in Figure 5, incubation of MCF-7 cells with 20 μM **4p** for 24 h resulted in a dramatic reduction of the proliferation rate. Only 14% of the cells were still able to synthesize DNA, a ratio that was further decreased after 48 h to 1.3% (not shown here). When **4p** was used at 100 μM, cell proliferation was completely inhibited even after a 24 h exposure. Staining of MCF-7 cells with **1** (Hoechst 33258, 4-{6-[6-(4-methylpiperazin-1-yl)-1*H*-1,3-benzodiazol-2-yl]-1*H*-1,3-benzodiazol-2-yl}-phenol)[43] indicated that the cells were markedly damaged after treatment with **4p** (Figure 4A). Already at 24 h of treatment, the entire number of MCF-7 cells underwent cell death and the total number of detectable cells was strongly reduced, down to 10%. The remaining cells showed characteristic features of apoptosis, such as reduction of nuclear size and condensation of chromatin (Figure 4A). In contrast, **1** staining did not indicate any sign of apoptosis after treatment with 20 μM **4p**. The nuclear morphology of cells under these conditions was similar to DMSO-treated control cells. This clearly indicated that the prenyl-substituted indeno[1,2-*b*]indole **4p** has a distinct antiproliferative effect at 20 μM concentration against MCF-7 breast cancer cells.

Inhibition of ABCG2-Mediated Drug Efflux. The same 16 indeno[1,2-*b*]indole derivatives were assayed for their ability to inhibit ABCG2-mediated mitoxantrone efflux from trans-

dx.doi.org/10.1021/jm500943z | J. Med. Chem. 2015, 58, 265−277

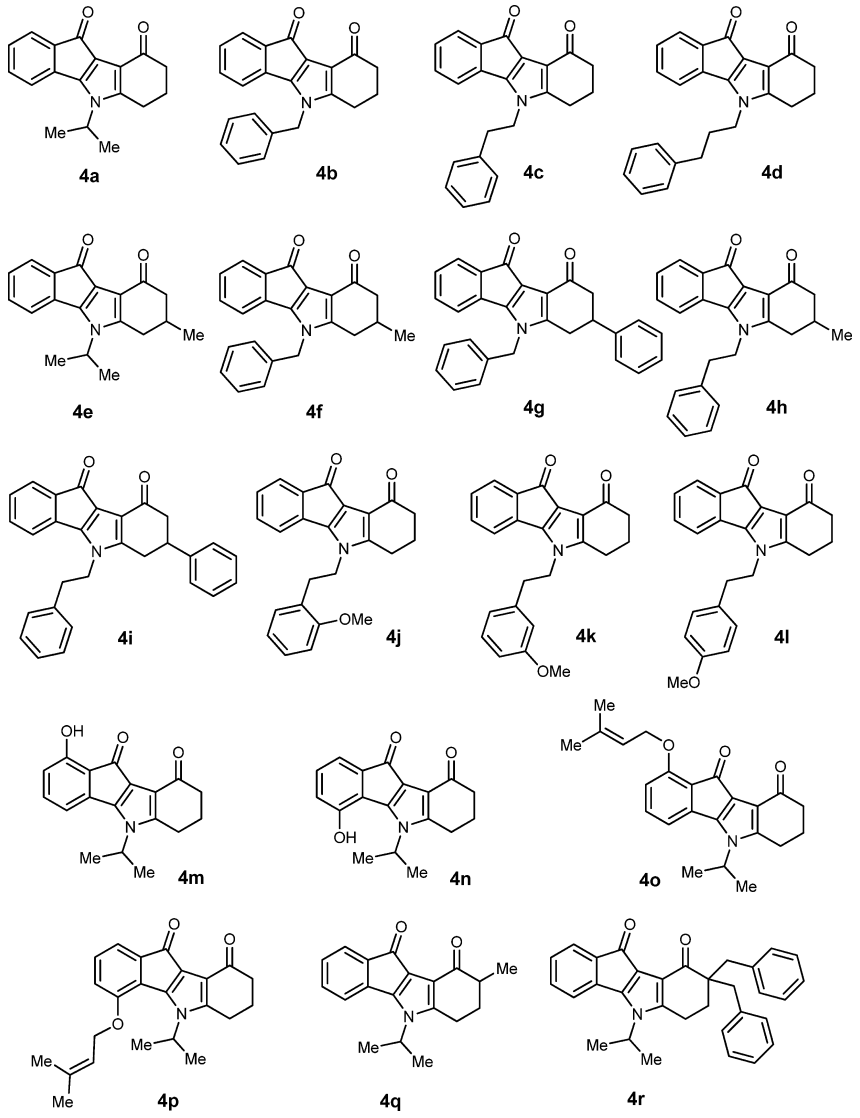

Figure 1. Substitution patterns of **4a**–**r**. Compounds **4a**–**d** and **4f**–**h** are described in ref 33, and compound **4e** is described in ref 37.

fected HEK293 cells. Table 2 shows that the worst CK2 inhibitors appear to be the best ABCG2 inhibitors. Indeed, the N^5-phenethyl substituted compounds produced a complete inhibition, with strong efficiency at submicromolar concentrations, as exemplified by **4c** (IC_{50} = 0.43 μM). A 2-fold further increase in potency was observed by methyl substitution at position 7 in **4h** or by methoxy substitution at phenethyl position ortho in **4j**, whereas an opposite, negative effect was produced at phenethyl position para in **4l** and an intermediate one at phenethyl position meta in **4k**.

The concentration dependence of the inhibition of ABCG2-mediated mitoxantrone efflux is illustrated for selected inhibitors in Figure 6.

Increasing the length of the N^5-substituent into phenpropyl in **4d** induced a moderate alteration (2-fold), whereas a dramatic loss of potency was produced by shortening into either benzyl in **4b** or isopropyl in **4a** (approximately 70- to 100-fold). A main part of this loss in potency could be recovered through hydrophobic substitution by two benzyl groups at position 8 in **4r** versus **4a**, while a partial recovery was observed at vicinal position 7 with either a phenyl group in **4g** versus **4b** or a methyl group in **4e** versus **4a**. A partial recovery of inhibition potency was observed with prenyl substitution not only at position 4 in **4p** but also at position 1 in **4o**, by comparison to **4a**. The best indenoindole inhibitors were nearly as potent as ABCG2 reference inhibitors, **2** (chromone 1) and **3** (Ko143), assayed under the same conditions.[44] In some cases, the maximal inhibition, as observed at 10 μM, was not complete (with maximal values of 60–83%) for hydrophobic derivatives such as **4d**, **4g**, **4i**, and **4p** (with log *P* values of 4.9–6.2) relative to a complete inhibition produced by **4c** and **4j** with a log *P* of 4.4 and may be partly related to lower water solubility, as suggested for other ABCG2 inhibitors.[45] However, the fact that **4j**, **4k**, and **4l** (with the same log *P* of 4.4) gave a variable maximal inhibition indicates that other parameters are critical for inhibition potency, in agreement with known polyspecificity of multidrug transporters, where the number and positions of hydrophobic substituents can modulate the orientation of binding and subsequent inhibition.

Studies of the intermolecular interactions between ABCG2 and diverse ligands have revealed three important chemical features: hydrogen-bond acceptor (HBA), hydrophobic part (HP), and aromatic ring system (ARS).[46,47] According to different possible combinations (0–3 HBA + 0–3 HP + 0–2

dx.doi.org/10.1021/jm500943z | J. Med. Chem. 2015, 58, 265–277

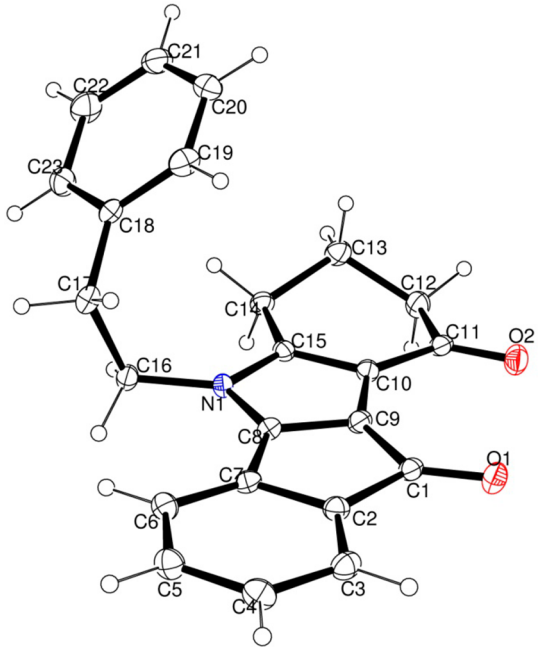

Figure 2. View of the crystal structure of **4c** with our numbering scheme. Displacement ellipsoids are drawn at the 30% probability level. The numbering used here is specific to the crystallographic studies and therefore different from that shown in Table 1 and used all along the text.

Table 1. Inhibition of Human CK2 Holoenzyme

	CK2 inhibition	
indenoindoles	% at 10 μM[a]	IC_{50} (μM)
4a	99	0.36[b]
4b	34	(~15)[c]
4c	59	7.0[b]
4d	62	6.0[b]
4e	94	0.17[b]
4f	16	(~35)[c]
4g	9	(~55)[c]
4h	66	2.5[b]
4i	35	(~15)[c]
4j	87	1.4[b]
4k	63	5.1[b]
4l	69	4.1[b]
4o	44	(~12)[c]
4p	100	0.025[b]
4q	52	9.2[b]
4r	48	(~11)[c]
ref inhibitors		
silmitasertib[d]	100	0.0037[b]
ellagic acid	95	0.04[b]
TBB[e]	99	0.06[b]
emodin	99	0.58[b]

[a]The percent inhibition of CK2 activity was determined for each compound at a fixed concentration of 10 μM. [b]For the best compounds producing at least 50% inhibition at 10 μM, the concentration was varied to precisely determine the IC_{50} values. [c]For the other, less potent compounds, a rough estimation was obtained from the experimental inhibition produced at 10 μM. [d]Silmitasertib = 5-[(3-chlorophenyl)amino]benzo[*c*][2,6]-naphthyridine-8-carboxylic acid. [e]TBB = 4,5,6,7-tetrabromo-benzotriazole.

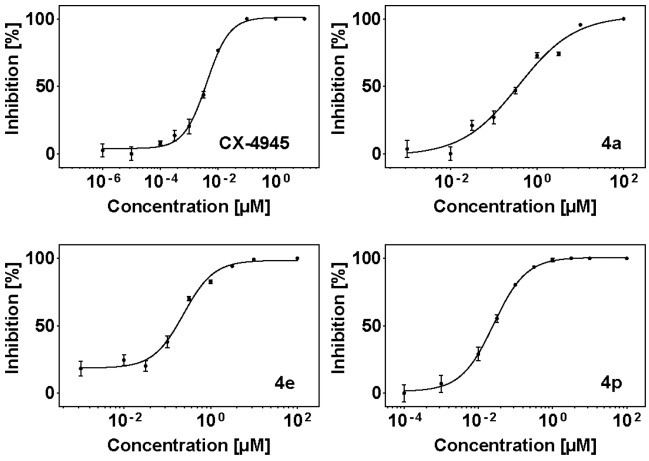

Figure 3. Concentration dependence for the most potent inhibitors of CK2 activity.

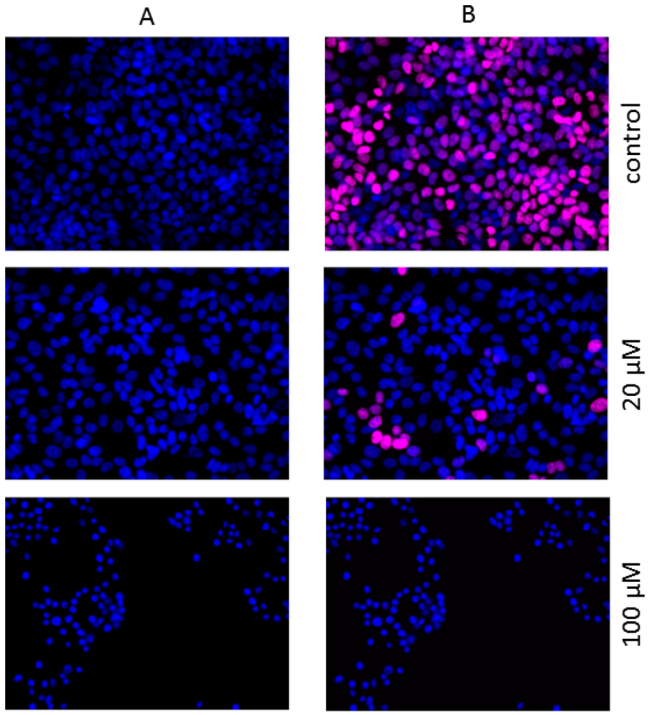

Figure 4. Fluorescence images of MCF-7 cells treated with different concentrations of the inhibitor **4p** for 24 h. Cell nuclei were double-stained by **1** (blue fluorescence), able to cross the membrane of all cells, and by EdU-assay using 5-TAMRA-PEG3-azide as a coupled fluorophore (violet fluorescence). Cell proliferation was monitored by EdU-assay. (A) Hoechst-staining of treated MCF-7 cells. (B) Overlay of the fluorescence images of **1** stained cells and TAMRA-labeled proliferating cells. The cells that are emitting only blue fluorescence are not proliferating, in contrast to those emitting an additional violet fluorescence.

ARS), various inhibition pharmacophores were designed. Interestingly, a given ligand may adopt different orientations to form its complex with ABCG2. Our lead compound **4h** is mainly characterized by 2 HBAs, 1 HP, and 3 ARSs and, according to different pharmacophore models, could indeed interact in variable orientations with the protein target. This point is closely related with the promiscuous nature of polyspecific multidrug transporters such as ABCG2.

dx.doi.org/10.1021/jm500943z | J. Med. Chem. 2015, 58, 265−277

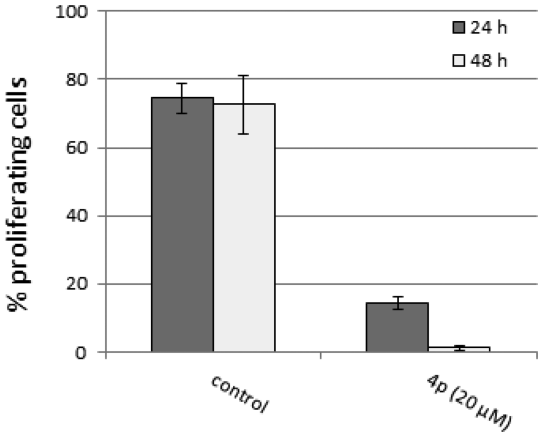

Figure 5. Antiproliferative effect of the inhibitor **4p** on MCF-7 cells. Results are shown as percent proliferating cells relative to control cells (with 1% DMSO) and represent the mean (±SD) of four assays.

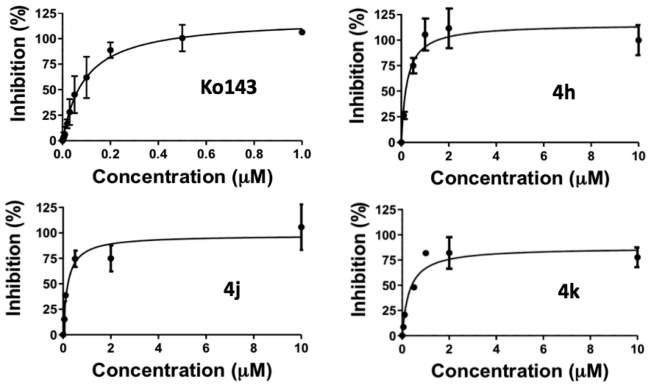

Figure 6. Concentration dependence for the most potent indenoindole inhibitors of ABCG2 transport activity.

Comparison in Table 2 of the relative ability of each compound to inhibit CK2 and ABCG2 indicates that the best CK2 inhibitors, with a N^5-isopropyl substituent, were about 2 orders of magnitude more selective for CK2 in **4a**, **4e**, and **4p** whereas the best ABCG2 inhibitors, with a N^5-phenethyl substituent, **4c**, **4h**, **4i**, **4j**, **4k**, and **4l**, were around 1 order of magnitude more selective for ABCG2. These differences are well illustrated in Figure 7A, also displaying that **4d**, with a longer N^5-substituent, and both **4r** and **4g**, with aromatic substituents on D-ring, were good ABCG2 inhibitors. By contrast, **4b**, **4f**, **4o**, and **4q** were only weak inhibitors of both CK2 and ABCG2, whereas no indenoindole derivative was found to potently inhibit both CK2 and ABCG2. Overall, 3 orders of magnitude in selectivity were separating the best ABCG2 inhibitors from the best CK2 inhibitors, despite them belonging to the same indeno[1,2-*b*]indole family of com-

Table 2. Inhibition of Mitoxantrone Efflux in ABCG2-Transfected Cells

	ABCG2 inhibition			cytotoxicity	
indenoindoles	% at 10 μM[a]	IC_{50} (μM)	ABCG2/CK2[d]	IG_{50} (μM)[e]	TR[f]
4a	15 ± 7	~35[c]	~0.01	nd	
4b	18 ± 3	~30[c]	~0.5	nd	
4c	100 ± 14	0.43 ± 0.01[b]	16	30.7 ± 9.5	71
4d	83 ± 25	0.79 ± 0.13[b]	8	>100	>127
4e	65 ± 17	4.1 ± 1.1[b]	~0.04	nd	
4f	33 ± 14	~15[c]	~2	nd	
4g	68 ± 10	0.96 ± 0.09[b]	~30	16.9 ± 6.5	18
4h	100 ± 21	0.23 ± 0.02[b]	11	>100	>435
4i	83 ± 13	0.49 ± 0.22[b]	~30	20.1 ± 4.9	96
4j	106 ± 22	0.21 ± 0.07[b]	7	27.2 ± 0.7	130
4k	78 ± 14	0.31 ± 0.09[b]	16	12.7 ± 3.1	41
4l	131 ± 6	0.70 ± 0.04[b]	6	68.5 ± 0.2	98
4o	74 ± 12	3.0 ± 0.5[b]	~4	nd	
4p	60 ± 26	1.6 ± 0.7[b]	0.02	31.0 ± 8.4	19
4q	40 ± 28	20 ± 14[b]	~0.46	nd	
4r	90 ± 20	0.61 ± 0.1[b]	~18	6.0 ± 1.0	10
ref inhibitors[g]					
chromone **1**[i]	98 ± 7	0.13 ± 0.09		96 ± 6	
Ko143[j]	106 ± 1	0.09 ± 0.01		32 ± 3	
ref substrates[h]					
mitoxantrone				0.009 ± 0.005	
SN-38[k]				0.005 ± 0.001	

[a]The percent inhibition of ABCG2-mediated mitoxantrone efflux was determined for each compound at a fixed concentration of 10 μM. [b]For the best compounds producing at least 50% inhibition at 10 μM, the concentration was varied to precisely determine the IC_{50} values. [c]For the other, less potent compounds, a rough estimation was obtained from the experimental inhibition produced at 10 μM. [d]The ABCG2/CK2 ratio, indicating the inhibitory efficiency of compounds toward ABCG2 relative to CK2, was calculated with the ratio between the IC_{50}(CK2) values from Table 2 and the IC_{50}(ABCG2) values. [e]The IG_{50} values of compounds cytotoxicity were determined after 72 h with MTT cell survival tests. nd, not determined. [f]The TR ratio was calculated by dividing the IG_{50} values of cytotoxicity by corresponding IC_{50} values of ABCG2 inhibition. [g]Other known inhibitors have been added for comparison with indenoindoles. [h]Cytotoxic substrates have been added for comparison with indenoindoles. [i]Chromone 1 = 5-[(4-bromobenzyl)oxy]-*N*-[2-(5-methoxy-1*H*-indol-3-yl)ethyl]-4-oxo-4*H*-chromene-2-carboxamide. [j]Ko143 = (3*S*,6*S*,12a*S*)-1,2,3,4,6,7,12,12a-octahydro-9-methoxy-6-(2-methylpropyl)-1,4-dioxopyrazino[1′,2′:1,6]pyrido[3,4-*b*]indole-3-propanoic acid 1,1-dimethylethyl ester. [k]SN-38 = 7-ethyl-10-hydroxycamptothecin, active metabolite of the topoisomerase I inhibitor irinotecan.

dx.doi.org/10.1021/jm500943z | J. Med. Chem. 2015, 58, 265−277

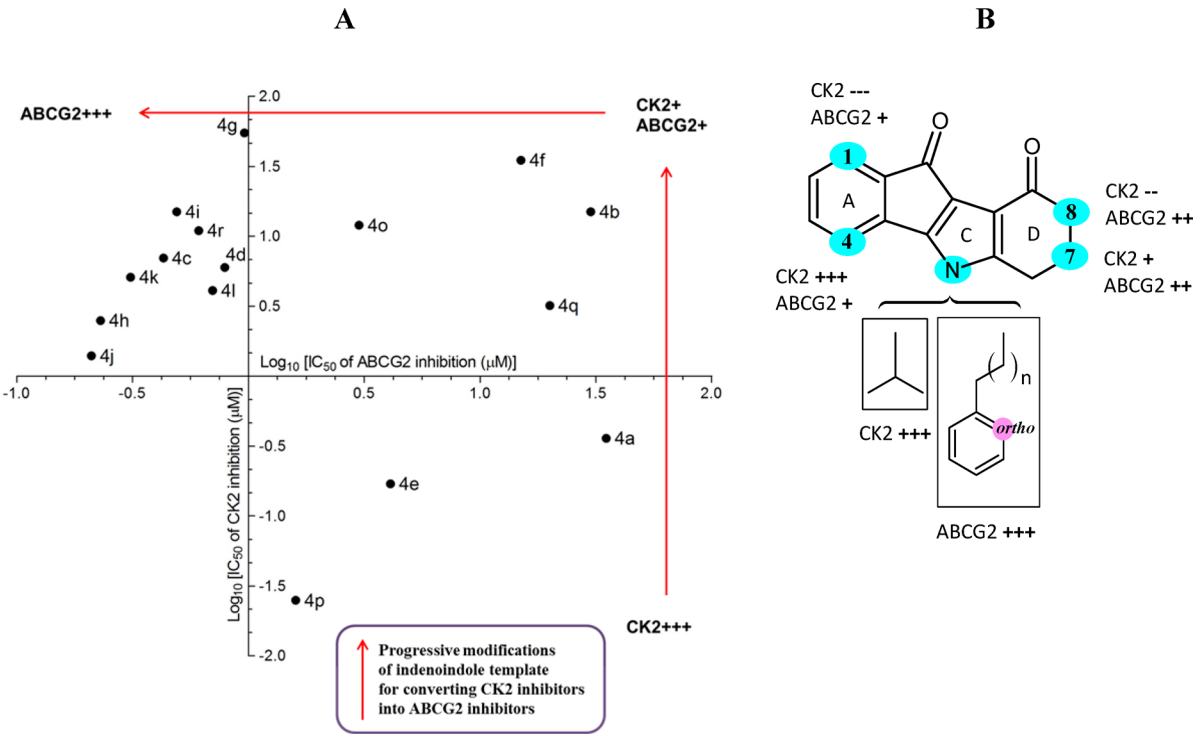

Figure 7. Relationships between CK2 inhibitors and ABCG2 inhibitors: (A) graphical representation as a function of relative IC_{50} values; (B) structural modifications of indenoindoles for exploring CK2 or ABCG2 inhibitors.

pounds, for example, **4c** and **4a** which only differ from the N^5-substitution.

Finally, Table 2 shows that among the best ABCG2 inhibitors, some displayed a very low cytotoxicity characterized by IG_{50} values higher than 100 μM, for **4h** and **4d**, or of 69 μM for **4l**, whereas other derivatives appeared more cytotoxic, such as **4r** (IG_{50} = 6 μM), and others were moderately cytotoxic such as **4k**, **4g**, **4j**, and **4c** (IG_{50} = 13−31 μM). A similar low or moderate cytotoxicity was observed with the reference inhibitors **2** and **3**, by difference with known cytotoxic substrates such as mitoxantrone and SN-38[18] (IG_{50} = 5−9 nM). For indenoindole inhibitors, comparison between cytotoxicity and potency of ABCG2 inhibition showed a very high therapeutic ratio, >435, for **4h**, compatible with future in vivo assays in animal models; three other derivatives, **4j**, **4l**, and **4d**, with a therapeutic ratio of around 100, might also be used. Some of the compounds displaying a moderate cytotoxicity, such as **4j** and **4h**, when assayed under 72 h cell survival MTT tests in both control HEK293 cells and ABCG2-transfected cells indicated no significant difference in IG_{50} values (not shown here); this indicated the absence of apparent ABCG2-mediated cross resistance, which suggested the absence of transport of the inhibitors.

Diverse structural modifications were performed on indeno-[1,2-*b*]indoles to design new CK2 inhibitors. The N^5-isopropyl derivative **4a** was progressively modified,[14,16,37] and the introduction of a prenyl group on position 4 of A-ring was extremely favorable (CK2+++, IC_{50} = 0.025 μM) (Figure 7A). Its analogue **4o**, with shifted substitution at position 1, gave significant information by (i) the emergence of ABCG2 inhibitory activity (ABCG2+) and (ii) the loss of CK2 inhibitory activity (CK2−). New pharmacomodulations allowed us to access to nine potent ABCG2 inhibitors (**4g**, **4d**, **4l**, **4r**, **4i**, **4c**, **4k**, **4j**, and **4h**) exhibiting submicromolar IC_{50} values (ABCG2+++).

The main structure−activity relationships of indeno[1,2-*b*]indoles for either CK2 inhibitors or ABCG2 inhibitors are schematically represented in Figure 7B. Quite interestingly, the different critical substitutions concerned the same positions, but generally with opposite effects of substituents, as following: (1) at N^5 position, the preferred substituent was isopropyl (20-fold over phenethyl) for CK2 inhibition, whereas phenethyl was the best (70- to 100-fold over benzyl and isopropyl) for ABCG2 inhibition; (2) at position 8, hydrophobic substitutions by a methyl and a set of two benzyl groups were highly negative (30-fold versus H) for CK2 inhibition, whereas they were highly positive (up to 60-fold) for ABCG2 inhibition; (3) at vicinal position 7, a hydrophobic phenyl was negative (3-fold versus H) for CK2 inhibition but quite positive (up to 30-fold) for ABCG2 inhibition. Position 7 for methyl substitution and phenethyl position ortho for methoxy substitution produced similar effects on both CK2 and ABCG2, namely, a 2- to 5-fold increase in potency. Prenyl substitution produced similar positive effects at position 4 (up to 20-fold increase in potency); however, it was highly selective for CK2 inhibition relative to position 1, by contrast to ABCG2 inhibition where a positive contribution was also observed. Finally, the ABCG2 inhibitory site appeared more hydrophobic and able to bind bigger indeno[1,2-*b*]indole derivatives than the CK2 inhibitory site. This fully agrees with the fact that the ABCG2 binding site is expected to be located in proximity to the hydrophobic drug-binding sites, as previously characterized for various heterocyclic inhibitors[31,32] and as recently reviewed,[48,49] by contrast to the CK2 inhibitory site which has been shown to widely overlap the hydrophilic ATP-binding site.[16]

dx.doi.org/10.1021/jm500943z | J. Med. Chem. 2015, 58, 265−277

EXPERIMENTAL SECTION

Chemistry. Melting points were determined on an Electrothermal 9200 capillary apparatus. The IR spectra were recorded on a PerkinElmer Spectrum Two IR spectrometer. The ^{1}H and ^{13}C NMR spectra were recorded at 400 MHz on a Bruker DRX 400 spectrometer. Chemical shifts are expressed in ppm (δ) downfield from internal tetramethylsilane, and coupling constants J are reported in hertz (Hz). The following abbreviations are used: s, singlet; bs, broad singlet; d, doublet; t, triplet; dd, doubled doublet; dt, doubled triplet; q, quartet; m, multiplet; Cquat, quaternary carbons. The mass spectra were performed by direct ionization (EI or CI) on a ThermoFinnigan MAT 95 XL apparatus. Chromatographic separations were performed on silica gel columns by column chromatography (Kieselgel 300−400 mesh). All reactions were monitored by TLC on GF254 plates that were visualized under a UV lamp (254 nm). Evaporation of solvent was performed in vacuum with rotating evaporator. The purity of the final compounds (greater than 95%) was determined by uHPLC/MS on an Agilent 1290 system using a Agilent 1290 Infinity ZORBAX Eclipse Plus C18 column (2.1 mm × 50 mm, 1.8 μm particle size) with a gradient mobile phase of H_2O/CH_3CN (90:10, v/v) with 0.1% of formic acid to H_2O/CH_3CN (10:90, v/v) with 0.1% of formic acid at a flow rate of 0.5 mL/min, with UV monitoring at the wavelength of 254 nm with a run time of 10 min.

General Procedure for the Synthesis of Compounds 2. A solution containing 10.62 mmol of primary amine and 10.62 mmol of the corresponding cyclohexane-1,3-dione dissolved in 60 mL of toluene was refluxed in a Dean−Stark trap until the separation of H_2O had finished. The solvent was then evaporated under vacuum and the resultant residue was taken up in EtOAc to give a yellow solid that was isolated by filtration. Further purification was then accomplished by silica gel column chromatography with CH_2Cl_2/acetone (1:3, v/v) as the eluent.

*5-Phenyl-3-(2-phenylethylamino)cyclohex-2-enone (**2i**).* Yellow solid. Yield 75%. Mp 117 °C. IR (ν cm^{-1}): 3240, 1698, 1660, 1601. ^{1}H NMR ($CDCl_3$, 400 MHz) δ: 7.33−7.20 (m, 10H, Harom), 5.30 (s, 1H, H-2), 5.00 (s, 1H, NH), 3.44−3.31 (m, 3H, H-5 and CH_2), 2.94 (t, 2H, J = 7.0 Hz, CH_2), 2.70−2.40 (m, 4H, 2 CH_2). ^{13}C NMR + DEPT ($CDCl_3$, 100 MHz) δ: 196.60 (C═O), 163.52 (Cquat), 143.41 (Cquat), 138.35 (Cquat), 129.11 (2 CH), 129.02 (2 CH), 128.93 (2 CH), 127.22 (CH), 127.12 (CH), 127.02 (2 CH), 96.97 (CH), 44.24 (CH_2), 43.79 (CH_2), 40.24 (CH), 37.57 (CH_2), 34.62 (CH_2). HRMS calcd for $C_{20}H_{22}NO$ $[M + H]^+$ 292.1696, found 292.1692.

*3-[2-(2-Methoxyphenyl)ethylamino]cyclohex-2-enone (**2j**).* Yellow solid. Yield 90%. Mp 105 °C. IR (ν cm^{-1}): 3253, 1600, 1569, 1533. ^{1}H NMR ($CDCl_3$, 400 MHz) δ: 7.22 (dt, 1H, J_1 = 1.7 Hz, J_2 = 8.2 Hz, Harom), 7.10 (dd, 1H, J_1 = 1.6 Hz, J_2 = 7.3 Hz, Harom), 6.92−6.86 (m, 2H, Harom), 5.15 (s, 1H, H-2), 5.1 (s, 1H, NH), 3.84 (s, 3H, OMe), 3.29 (m, 2H, CH_2), 2.89 (t, 2H, J = 6.8 Hz, CH_2), 2.29−2.24 (m, 4H, 2 CH_2), 1.93 (m, 2H, CH_2). ^{13}C NMR + DEPT ($CDCl_3$, 100 MHz) δ: 197.43 (C═O), 164.50 (Cquat), 157.64 (Cquat), 130.85 (CH), 128.46 (CH), 127.21 (Cquat), 121.21 (CH), 110.78 (CH), 96.98 (CH), 55.57 (CH_3), 43.59 (CH_2), 36.71 (CH_2), 30.14 (CH_2), 29.59 (CH_2), 22.28 (CH_2). HRMS calcd for $C_{15}H_{20}NO_2$ $[M + H]^+$ 246.1489, found 246.1489.

*3-[2-(3-Methoxyphenyl)ethylamino]cyclohex-2-enone (**2k**).* Beige solid. Yield 80%. Mp 94 °C. IR (ν cm^{-1}): 3256, 1601, 1570, 1531. ^{1}H NMR ($CDCl_3$, 400 MHz) δ: 7.22 (t, 1H, J = 7.9 Hz, Harom), 6.79−6.75 (m, 2H, Harom), 6.71 (m, 1H, Harom), 5.17 (s, 1H, H-2), 4.73 (s, 1H, NH), 3.79 (s, 3H, OMe), 3.44 (m, 2H, CH_2), 2.85 (t, 2H, J = 7.0 Hz, CH_2), 2.31−2.26 (m, 4H, 2 CH_2), 1.93 (m, 2H, CH_2). ^{13}C NMR + DEPT ($CDCl_3$, 100 MHz) δ: 197.63 (C═O), 164.36 (Cquat), 160.20 (Cquat), 140.04 (Cquat), 130.11 (CH), 121.22 (CH), 114.77 (CH), 112.24 (CH), 97.36 (CH), 55.51 (CH_3), 43.91 (CH_2), 36.75 (CH_2), 34.67 (CH_2), 30.11 (CH_2), 22.60 (CH_2). HRMS calcd for $C_{15}H_{20}NO_2$ $[M + H]^+$ 246.1489, found 246.1494.

*3-[2-(4-Methoxyphenyl)ethylamino]cyclohex-2-enone (**2l**).* Yellow solid. Yield 90%. Mp 89 °C. IR (ν cm^{-1}): 3247, 1596, 1531, 1511. ^{1}H NMR ($CDCl_3$, 400 MHz) δ: 7.08 (d, 2H, J = 8.6 Hz, Harom), 6.84 (d, 2H, J = 8.6 Hz, Harom), 5.16 (s, 1H, H-2), 4.79 (s, 1H, NH), 3.78 (s, 3H, OMe), 3.30 (m, 2H, CH_2), 2.82 (t, 2H, J = 7.0 Hz, CH_2), 2.30−2.26 (m, 4H, 2 CH_2), 1.93 (m, 2H, CH_2). ^{13}C NMR + DEPT ($CDCl_3$, 100 MHz) δ: 197.54 (C═O), 164.43 (Cquat), 158.74 (Cquat), 130.37 (Cquat), 129.88 (2 CH), 114.47 (2 CH), 97.28 (CH), 55.57 (CH_3), 44.24 (CH_2), 36.75 (CH_2), 30.77 (CH_2), 30.08 (CH_2), 22.26 (CH_2). HRMS calcd for $C_{15}H_{20}NO_2$ $[M + H]^+$ 246.1489, found 246.1483.

General Procedure for the Synthesis of Compounds 3. A solution containing 6.86 mmol of enaminone **2** and 6.86 mmol of ninhydrin dissolved in 25 mL of MeOH was stirred at room temperature for 8 h. Generally, a precipitate of compound **3** was formed. It was recovered and washed with MeOH. A second quantity was obtained from the filtrate by purification by silica gel column chromatography with CH_2Cl_2/acetone (1:3, v/v) as the eluent.

*4b,9b-Dihydroxy-7-phenyl-5-(2-phenylethyl)-4b,5,6,7,8,9b-hexahydroindeno[1,2-b]indole-9,10-dione (**3i**).* White solid. Yield 84%. Mp 128 °C. IR (ν cm^{-1}): 3471, 1714, 1603, 1521. ^{1}H NMR ($CDCl_3$, 400 MHz) δ: 7.95−7.87 (m, 2H, Harom), 7.77 (m, 1H, Harom), 7.57 (m, 1H, Harom), 7.36−7.20 (m, 8H, Harom), 7.09−7.03 (m, 2H, Harom), 4.11 (m, 1H, NCH_2), 3.82 (m, 1H, NCH_2), 3.25 (m, 1H, $\underline{CH_2}$Ph), 3.11 (m, 1H, H-7), 2.99 (m, 1H, $\underline{CH_2}$Ph), 2.61−2.11 (m, 4H, CH_2-6 and CH_2-8). ^{13}C NMR + DEPT ($CDCl_3$, 100 MHz) δ: 197.78 (d, C═O), 191.10 (d, C═O), 166.84 (d, Cquat), 148.51 (d, Cquat), 143.01 (d, Cquat), 138.70 (d, Cquat), 136.10 (d, CH), 135.52 (d, Cquat), 130.80 (d, CH), 129.51 (d, 2 CH), 129.20 (d, 2 CH), 128.99 (d, 2 CH), 127.32 (d, 2 CH), 127.12 (d, 2 CH), 125.12 (d, CH), 124.52 (d, CH), 105.37 (d, Cquat), 96.87 (d, Cquat), 83.12 (d, Cquat), 44.88 (d, CH_2), 44.11 (d, CH_2), 40.42 (d, CH), 37.83 (s, CH_2), 30.84 (d, CH_2). HRMS calcd for $C_{29}H_{26}NO_4$ $[M + H]^+$ 452.1856, found 452.1840.

*4b,9b-Dihydroxy-5-[2-(2-methoxyphenyl)ethyl]-4b,5,6,7,8,9b-hexahydroindeno[1,2-b]indole-9,10-dione (**3j**).* Yellow solid. Yield 93%. Mp 114 °C. IR (ν cm^{-1}): 3465, 1716, 1656, 1601, 1524. ^{1}H NMR ($CDCl_3$, 400 MHz) δ: 7.92 (d, 1H, J = 7.8 Hz, Harom), 7.85 (d, 1H, J = 7.6 Hz, Harom), 7.73 (m, 1H, Harom), 7.54 (m, 1H, Harom), 7.26 (m, 1H, Harom), 7.16 (dd, 1H, J_1 = 1.7 Hz, J_2 = 7.4 Hz, Harom), 6.94 (m, 1H, Harom), 6.89 (d, 1H, J = 8.2 Hz, Harom), 4.88 (bs, 1H, OH), 3.98 (m, 1H, NCH_2), 3.77 (m, 1H, NCH_2), 3.13 (m, 1H, $\underline{CH_2}$Ph), 2.98 (m, 1H, $\underline{CH_2}$Ph), 2.38 (bs, 1H, OH), 2.22 (m, 2H, CH_2), 2.16 (m, 2H, CH_2), 1.84 (m, 1H, CH_2), 1.73 (m, 1H, CH_2). ^{13}C NMR + DEPT ($CDCl_3$, 100 MHz) δ: 198.11 (C═O), 192.39 (C═O), 167.26 (Cquat), 157.84 (Cquat), 148.42 (Cquat), 136.05 (CH), 135.44 (Cquat), 131.28 (CH), 130.75 (CH), 128.83 (CH), 126.71 (Cquat), 125.13 (CH), 124.43 (CH), 121.31 (CH), 110.81 (CH), 105.53 (Cquat), 96.22 (Cquat), 83.01 (Cquat), 55.84 (CH_3), 43.29 (CH_2), 36.64 (CH_2), 32.90 (CH_2), 23.16 (CH_2), 21.88 (CH_2). HRMS calcd for $C_{24}H_{24}NO_5$ $[M + H]^+$ 406.1649, found 406.1641.

*4b,9b-Dihydroxy-5-[2-(3-methoxyphenyl)ethyl]-4b,5,6,7,8,9b-hexahydroindeno[1,2-b]indole-9,10-dione (**3k**).* White solid. Yield 94% yield. Mp 95 °C. IR (ν cm^{-1}): 3471, 1713, 1655, 1599, 1521. ^{1}H NMR (DMSO-d_6, 400 MHz) δ: 8.04 (d, 1H, J = 7.8 Hz, Harom), 7.84 (m, 1H, Harom), 7.74 (d, 1H, J = 7.5 Hz, Harom), 7.62 (m, 1H, Harom), 7.29 (m, 1H, Harom), 6.95−6.92 (m, 2H, Harom), 6.90 (bs, 1H, OH), 6.85 (dd, 1H, J_1 = 2.6 Hz, J_2 = 8.2 Hz, Harom), 5.79 (bs, 1H, OH), 4.01 (m, 1H, NCH_2), 3.75 (m, 1H, NCH_2), 3.40 (s, 3H, OMe), 2.97 (m, 2H, $\underline{CH_2}$Ph), 2.24 (m, 2H, CH_2), 2.05 (m, 2H, CH_2), 1.73 (m, 1H, CH_2), 1.65 (m, 1H, CH_2). ^{13}C NMR + DEPT (DMSO-d_6, 100 MHz) δ: 198.58 (C═O), 189.68 (C═O), 166.22 (Cquat), 160.36 (Cquat), 149.19 (Cquat), 141.49 (Cquat), 136.53 (CH), 135.73 (Cquat), 131.20 (CH), 130.51 (CH), 125.74 (CH), 124.11 (CH), 122.19 (CH), 115.52 (CH), 113.00 (CH), 105.71 (Cquat), 96.60 (Cquat), 84.54 (Cquat), 55.99 (CH_3), 44.37 (CH_2), 37.93 (CH_2), 37.84 (CH_2), 23.24 (CH_2), 22.33 (CH_2). HRMS calcd for $C_{24}H_{24}NO_5$ $[M + H]^+$ 406.1649, found 406.1658.

*4b,9b-Dihydroxy-5-[(2-(4-methoxyphenyl)ethyl]-4b,5,6,7,8,9b-hexahydroindeno[1,2-b]indole-9,10-dione (**3l**).* Yellow solid. Yield 97%. Mp 116 °C. IR (ν cm^{-1}): 3489, 1713, 1660, 1605, 1577, 1539, 1509. ^{1}H NMR ($CDCl_3$, 400 MHz) δ: 7.89−7.84 (m, 2H, Harom), 7.73 (m, 1H, Harom), 7.54 (m, 1H, Harom), 7.13−7.10 (m, 2H, Harom), 6.89−6.85 (m, 2H, Harom), 5.53 (bs, 1H, OH), 5.14 (bs,

dx.doi.org/10.1021/jm500943z | J. Med. Chem. 2015, 58, 265−277

1H, OH), 3.99 (m, 1H, NCH_2), 3.80 (s, 3H, OMe), 3.72 (m, 1H, NCH_2), 2.99 (m, 2H, $\underline{CH_2}Ph$), 2.23 (m, 2H, CH_2), 2.12 (m, 2H, CH_2), 1.87 (m, 1H, CH_2), 1.71 (m, 1H, CH_2). ^{13}C NMR + DEPT ($CDCl_3$, 100 MHz) δ: 197.88 (C=O), 192.44 (C=O), 167.17 (Cquat), 158.92 (Cquat), 148.53 (Cquat), 136.04 (CH), 135.49 (Cquat), 130.73 (CH), 130.62 (Cquat), 130.32 (2 CH), 125.16 (CH), 124.43 (CH), 114.60 (2 CH), 105.64 (Cquat), 96.22 (Cquat), 83.19 (Cquat), 55.68 (CH_3), 45.02 (CH_2), 36.97 (CH_2), 36.59 (CH_2), 23.35 (CH_2), 21.82 (CH_2). HRMS calcd for $C_{24}H_{24}NO_5$ $[M + H]^+$ 406.1649, found 406.1638.

General Procedure for the Synthesis of Compounds 4i–n. A solution containing 4.43 mmol of **3** and 8.86 mmol (2 equiv) of TETA dissolved in 15 mL of DMF and 2.5 mL of AcOH was stirred at room temperature for 22 h. The solution was then poured into 300 mL of ice and water and stirred for 1 h. The resulting precipitate was filtered and washed with water and dried to give a first quantity of **4**. The filtrate was evaporated and the residue was diluted with H_2O. The solution was basified with $NaHCO_3$ and extracted with CH_2Cl_2. The organic phase was dried over anhydrous Na_2SO_4 and evaporated in vacuum to give a second quantity of **4** which was purified by silica gel column chromatography with CH_2Cl_2/acetone (95:5, v/v) as the eluent.

*7-Phenyl-5-(2-phenylethyl)-5,6,7,8-tetrahydroindeno[1,2-b]-indole-9,10-dione (**4i**).* Orange solid. Yield 95%. Mp 228 °C. IR (ν cm^{-1}): 1698, 1660, 1603, 1520. ^1H NMR ($CDCl_3$, 400 MHz) δ: 7.47 (d, 1H, J = 6.8 Hz, Harom), 7.33–7.22 (m, 7H, Harom), 7.14 (m, 1H, Harom), 7.07 (d, 2H, J = 7.0 Hz, Harom), 6.98–6.93 (m, 3H, Harom), 4.15 (m, 2H, NCH_2), 3.08–3.00 (m, 3H, H-7 and $\underline{CH_2}Ph$), 2.60 (dd, 1H, J_1 = 4.0 Hz, J_2 = 16.4 Hz, H-6 or H-8), 2.51 (dd, 1H, J_1 = 12.6 Hz, J_2 = 16.4 Hz, H-6 or H-8), 2.25 (dd, 1H, J_1 = 4.8 Hz, J_2 = 16.4 Hz, H-6 or H-8), 2.10 (dd, 1H, J_1 = 11.6 Hz, J_2 = 16.4 Hz, H-6 or H-8). ^{13}C NMR + DEPT ($CDCl_3$, 100 MHz) δ: 191.47 (C=O), 184.55 (C=O), 152.81 (Cquat), 150.27 (Cquat), 142.97 (Cquat), 139.04 (Cquat), 137.01 (Cquat), 135.09 (Cquat), 132.75 (CH), 129.43 (2 CH), 129.30 (2 CH), 128.99 (2 CH), 128.73 (CH), 127.76 (CH), 127.38 (CH), 127.01 (2 CH), 124.16 (CH), 120.39 (Cquat), 117.42 (CH), 117.16 (Cquat), 47.76 (CH_2), 44.90 (CH_2), 41.64 (CH), 37.22 (CH_2), 29.94 (CH_2). HRMS calcd for $C_{29}H_{24}NO_2$ $[M + H]^+$ 418.1802, found 418.1791.

*5-[2-(2-Methoxyphenyl)ethyl]-5,6,7,8-tetrahydroindeno[1,2-b]-indole-9,10-dione (**4j**).* Orange solid. Yield 83%. Mp 198 °C. IR (ν cm^{-1}): 1698, 1664, 1605, 1531. ^1H NMR ($CDCl_3$, 400 MHz) δ: 7.40 (d, 1H, J = 7.0 Hz, Harom), 7.22–7.17 (m, 2H, Harom), 7.08 (m, 1H, Harom), 6.98 (d, 1H, J = 7.1 Hz, Harom), 6.90 (d, 1H, J = 6.4 Hz, Harom), 6.83–6.79 (m, 2H, Harom), 4.12 (t, 2H, J = 6.9 Hz, NCH_2), 3.79 (s, 3H, OMe), 3.06 (t, 2H, J = 6.9 Hz, $\underline{CH_2}Ph$), 2.34 (m, 2H, CH_2-6 or CH_2-8), 2.27 (m, 2H, CH_2-6 or CH_2-8), 1.90 (m, 2H, CH_2-7). ^{13}C NMR + DEPT ($CDCl_3$, 100 MHz) δ: 192.63 (C=O), 184.63 (C=O), 157.73 (Cquat), 153.04 (Cquat), 150.91 (Cquat), 139.08 (Cquat), 135.25 (Cquat), 132.53 (CH), 131.05 (CH), 129.15 (CH), 128.49 (CH), 125.05 (Cquat), 123.92 (CH), 121.14 (CH), 120.06 (Cquat), 117.52 (Cquat), 117.36 (CH), 110.54 (CH), 55.57 (CH_3), 46.08 (CH_2), 38.05 (CH_2), 32.16 (CH_2), 23.28 (CH_2), 21.74 (CH_2). HRMS calcd for $C_{24}H_{22}NO_3$ $[M + H]^+$ 372.1594, found 372.1590.

*5-[2-(3-Methoxyphenyl)ethyl]-5,6,7,8-tetrahydroindeno[1,2-b]-indole-9,10-dione (**4k**).* Orange solid. Yield 60%. Mp 176 °C. IR (ν cm^{-1}): 1696, 1661, 1594. ^1H NMR ($CDCl_3$, 400 MHz) δ: 7.43 (dd, 1H, J_1 = 0.6 Hz, J_2 = 7.1 Hz, Harom), 7.22–7.08 (m, 3H, Harom), 6.88 (d, 1H, J = 7.1 Hz, Harom), 6.75 (m, 1H, Harom), 6.57 (d, 1H, J = 7.6 Hz, Harom), 6.49 (m, 1H, Harom), 4.14 (t, 2H, J = 6.5 Hz, NCH_2), 3.69 (s, 3H, OMe), 3.03 (t, 2H, J = 6.5 Hz, $\underline{CH_2}Ph$), 2.33 (m, 2H, CH_2-6 or CH_2-8), 2.09 (m, 2H, CH_2-6 or CH_2-8), 1.85 (m, 2H, CH_2-7). ^{13}C NMR + DEPT ($CDCl_3$, 100 MHz) δ: 192.58 (C=O), 184.54 (C=O), 160.25 (Cquat), 152.53 (Cquat), 151.04 (Cquat), 139.07 (Cquat), 138.50 (Cquat), 135.12 (Cquat), 132.63 (CH), 130.35 (CH), 128.65 (CH), 124.14 (CH), 121.45 (CH), 120.47 (Cquat), 117.60 (Cquat), 117.27 (CH), 114.86 (CH), 113.01 (CH), 55.54 (CH_3), 47.71 (CH_2), 38.02 (CH_2), 37.29 (CH_2), 23.22 (CH_2), 21.90 (CH_2). HRMS calcd for $C_{24}H_{22}NO_3$ $[M + H]^+$ 372.1594, found 372.1601.

*5-[2-(4-Methoxyphenyl)ethyl]-5,6,7,8-tetrahydroindeno[1,2-b]-indole-9,10-dione (**4l**).* Orange solid. Yield 87%. Mp 181 °C. IR (ν cm^{-1}): 1697, 1660, 1605, 1511. ^1H NMR ($CDCl_3$, 400 MHz) δ: 7.44 (d, 1H, J = 7.1 Hz, Harom), 7.20 (m, 1H, Harom), 7.11 (m, 1H, Harom), 6.90–6.87 (m, 3H, Harom), 6.79–6.76 (m, 2H, Harom), 4.12 (t, 2H, J = 6.5 Hz, NCH_2), 3.73 (s, 3H, OMe), 3.01 (t, 2H, J = 6.5 Hz, $\underline{CH_2}Ph$), 2.33 (m, 2H, CH_2-6 or CH_2-8), 2.10 (m, 2H, CH_2-6 or CH_2-8), 1.85 (m, 2H, CH_2-7). ^{13}C NMR + DEPT ($CDCl_3$, 100 MHz) δ: 192.65 (C=O), 184.60 (C=O), 159.31 (Cquat), 152.54 (Cquat), 150.96 (Cquat), 139.11 (Cquat), 135.17 (Cquat), 132.61 (CH), 130.31 (2 CH), 128.88 (Cquat), 128.65 (CH), 124.16 (CH), 120.52 (Cquat), 117.62 (Cquat), 117.28 (CH), 114.65 (2 CH), 55.67 (CH_3), 47.96 (CH_2), 38.04 (CH_2), 36.39 (CH_2), 23.26 (CH_2), 21.95 (CH_2). HRMS calcd for $C_{24}H_{21}NNaO_3$ $[M + Na]^+$ 394.1414, found 394.1403.

*1-Hydroxy-5-isopropyl-5,6,7,8-tetrahydroindeno[1,2-b]indole-9,10-dione (**4m**).* Orange solid. Yield 81%. Mp 167 °C. IR (ν cm^{-1}): 3214, 1696, 1672, 1623. ^1H NMR (DMSO-d_6, 400 MHz) δ: 9.74 (s, 1H, OH), 7.22 (m, 1H, H-3), 6.91 (d, 1H, J = 7.3 Hz, H-4), 6.71 (d, 1H, J = 8.5 Hz, H-2), 4.74 (m, 1H, $\underline{CH}Me_2$), 2.93 (t, 2H, J = 5.6 Hz, CH_2-6 or CH_2-8), 2.35 (t, 2H, J = 5.8 Hz, CH_2-6 or CH_2-8), 2.06 (m 2H, CH_2-7), 1.54 (d, 6H, J = 9.3 Hz, $CH\underline{Me_2}$). ^{13}C NMR + DEPT (DMSO-d_6, 100 MHz) δ: 192.25 (C=O), 185.44 (C=O), 156.24 (2 Cquat), 151.19 (Cquat), 150.40 (Cquat), 136.57 (Cquat), 135.64 (CH), 120.62 (CH), 120.14 (Cquat), 117.56 (Cquat), 113.15 (CH), 50.02 (CH), 38.58 (2 CH_2), 23.75 (CH_2), 22.15 (2 CH_3). HRMS calcd for $C_{18}H_{17}NNaO_3$ $[M + Na]^+$ 318.1101, found 318.1094.

*4-Hydroxy-5-isopropyl-5,6,7,8-tetrahydroindeno[1,2-b]indole-9,10-dione (**4n**).* Pink solid. Yield 19%. Mp 309 °C. IR (ν cm^{-1}): 2642, 1698, 1596. ^1H NMR (DMSO-d_6, 400 MHz) δ: 10.58 (s, 1H, OH), 7.08 (m, 1H, H-2), 6.92 (d, 1H, J = 8.3 Hz, H-1 or H-3), 6.89 (d, 1H, J = 6.8 Hz, H-1 or H-3), 5.91 (m, 1H, $\underline{CH}Me_2$), 2.93 (t, 2H, J = 5.7 Hz, CH_2-6), 2.38 (t, 2H, J = 6.1 Hz, CH_2-8), 2.07 (m, 2H, CH_2-7), 1.56 (d, 6H, J = 6.8 Hz, $CH\underline{Me_2}$). ^{13}C NMR + DEPT (DMSO-d_6, 100 MHz) δ: 191.33 (C=O), 183.21 (C=O), 149.75 (Cquat), 147.94 (Cquat), 140.20 (Cquat), 131.60 (Cquat), 131.51 (Cquat), 130.00 (CH), 128.64 (Cquat), 123.40 (CH), 118.61 (Cquat), 115.10 (CH), 50.66 (CH), 41.42 (CH_2), 37.68 (2 CH_2), 21.60 (2 CH_3). HRMS calcd for $C_{18}H_{18}NO_3$ $[M + H]^+$ 296.1281, found 296.1279.

5-Isopropyl-1-(3-methylbut-2-enyloxy)-5,6,7,8-tetrahydroindeno[1,2-*b*]indole-9,10-dione (4o). A mixture of 1-hydroxyindenoindole **4m** (1 mmol), K_2CO_3 (3 mmol), and prenyl bromide (1.5 mmol) in DMA was heated at 80 °C for 24 h. The mixture was then poured into H_2O and extracted with CH_2Cl_2. The organic layers were washed with H_2O, dried over Na_2SO_4, filtered, and concentrated. The residue was purified by flash chromatography using acetone/CH_2Cl_2 (2:10, v/v) as the eluent to provide compound **4o**. Orange solid. Yield 27%. Mp 212 °C. IR (ν cm^{-1}): 1698, 1659, 1588, 1503. ^1H NMR ($CDCl_3$, 400 MHz) δ: 7.17 (m, 1H, H-3), 6.77 (d, 1H, J = 7.3 Hz, H-2 or H-4), 6.73 (d, 1H, J = 8.6 Hz, H-2 or H-4), 5.49 (m, 1H, $Me_2C{=}\underline{CH}$), 4.67 (d, 2H, J = 6.5 Hz, OCH_2), 4.61 (m, 1H, $\underline{CH}Me_2$), 2.83 (t, 2H, J = 6.0 Hz, CH_2-6 or CH_2-8), 2.46 (t, 2H, J = 5.8 Hz, CH_2-6 or CH_2-8), 2.14 (m, 2H, CH_2-7), 1.73 (d, 3H, J = 1.0 Hz, $\underline{Me_2}C{=}CH$), 1.71 (s, 3H, $\underline{Me_2}C{=}CH$), 1.62 (d, 6H, J = 7.1 Hz, $CH\underline{Me_2}$). ^{13}C NMR + DEPT ($CDCl_3$, 100 MHz) δ: 192.30 (C=O), 183.33 (C=O), 157.24 (Cquat), 149.61 (Cquat), 148.91 (Cquat), 138.06 (Cquat), 137.99 (Cquat), 134.10 (CH), 123.87 (Cquat), 121.64 (Cquat), 120.20 (CH), 117.90 (Cquat), 117.46 (CH), 112.71 (CH), 66.90 (CH_2), 49.60 (CH), 38.18 (CH_2), 26.07 (CH_3), 23.95 (CH_2), 23.61 (CH_2), 22.13 (2 CH_3), 18.67 (CH_3). HRMS calcd for $C_{23}H_{25}NNaO_3$ $[M + Na]^+$, 386.1727, found 386.1711.

5-Isopropyl-4-(3-methylbut-2-enyloxy)-5,6,7,8-tetrahydroindeno[1,2-*b*]indole-9,10-dione (4p). A solution of 4-hydroxyindenoindole **4n** (0.677 mmol, 1 equiv), K_2CO_3 (2.03 mmol, 3 equiv), and prenyl bromide (2.03 mmol, 3 equiv) in acetone (20 mL) was refluxed for 8 h. The mixture was then filtered and concentrated. The residue was purified by flash chromatography using acetone/CH_2Cl_2 (2:10, v/v) as the eluent to provide compound (**4p**). Red solid. Yield 60%. Mp 167 °C. IR (ν cm^{-1}): 1694, 1660, 1642, 1598. ^1H NMR (DMSO-d_6, 400 MHz) δ: 7.20–7.18 (m, 2H, H-1 and H-3), 6.98 (m, 1H, H-2), 5.84 (bs, 1H, $Me_2C{=}\underline{CH}$), 5.52 (m, 1H, $\underline{CH}Me_2$),

dx.doi.org/10.1021/jm500943z | J. Med. Chem. 2015, 58, 265–277

4.68 (d, 2H, J = 7.1 Hz, OCH_2), 2.98 (t, 2H, J = 5.87 Hz, CH_2-6 or CH_2-8), 2.37 (t, 2H, J = 5.74 Hz, CH_2-6 or CH_2-8), 2.06 (m, 2H, CH_2-7), 1.82 (s, 3H, $\underline{Me}_2C{=}CH$), 1.77 (d, 3H, J = 0.9 Hz, $\underline{Me}_2C{=}CH$), 1.49 (d, 6H, J = 7.1 Hz, $CH\underline{Me}_2$). ^{13}C NMR + DEPT (DMSO-d_6, 100 MHz) δ: 192.30 (C=O), 184.03 (C=O), 154.19 (Cquat), 151.07 (Cquat), 150.01 (Cquat), 140.61 (Cquat), 140.28 (Cquat), 131.35 (CH), 122.29 (Cquat), 120.86 (CH), 119.57 (CH), 119.12 (Cquat), 118.66 (Cquat), 117.10 (CH), 66.13 (CH_2), 51.74 (CH), 38.65 (CH_2), 26.42 (CH_3), 25.37 (CH_2), 24.31 (CH_2), 22.47 (2 CH_3), 18.88 (CH_3). HRMS calcd for $C_{23}H_{25}NNaO_3$ $[M + Na]^+$ 386.1727, found 386.1718.

General Procedure for the Synthesis of Compounds 4q and 4r. A solution of **4a** (1.79 mmol, 1 equiv) in dry THF (10 mL) was added dropwise under argon to a solution of LCIA prepared from cyclohexylisopropylamine (2 equiv) and n-BuLi (2.82 equiv) in dry THF (4.2 mL) at −20 °C. The resulting solution was cooled at −40 °C and stirred for 5 h. Then alkylating agent (16 equiv) was added dropwise and stirring was continued at −40 °C for 2 h. The reaction mixture was warmed to room temperature and stirred overnight. After the addition of 2 M HCl (4 mL), the reaction mixture was extracted with AcOEt. The combined organic layers were washed with water and brine successively and dried over anhydrous Na_2SO_4. The solvent was then evaporated under vacuum and the resultant residue was purified by silica gel column chromatography using EtOAc/cyclohexane (1:1, v/v) as the eluent.

*5-Isopropyl-8-methyl-5,6,7,8-tetrahydroindeno[1,2-b]indole-9,10-dione (**4q**).* Orange solid. Yield 10%. Mp 209 °C. IR (ν cm^{-1}): 1702, 1665, 1601, 1525. ^{1}H NMR ($CDCl_3$, 400 MHz) δ: 7.45 (m, 1H, Harom), 7.22 (m, 1H, Harom), 7.12−7.08 (m, 2H, Harom), 4.59 (m, 1H, $C\underline{H}Me_2$), 2.87 (m, 2H, CH_2-6), 2.47 (m, 1H, H-7), 2.22 (m, 1H, H-7), 1.90 (m, 1H, H-8), 1.63 (d, 3H, J = 7.0 Hz, $CH\underline{Me}_2$), 1.64 (d, 3H, J = 7.0 Hz, $CH\underline{Me}_2$), 1.21 (d, 3H, J = 7.0 Hz, CH_3-8). ^{13}C NMR + DEPT ($CDCl_3$, 100 MHz) δ: 194.87 (C=O), 184.54 (C=O), 152.00 (Cquat), 148.58 (Cquat), 139.32 (Cquat), 135.76 (Cquat), 132.40 (CH), 128.41 (CH), 124.14 (CH), 121.11 (Cquat), 118.97 (CH), 117.74 (Cquat), 49.57 (CH), 41.56 (CH), 31.51 (CH_2), 23.19 (CH_2), 22.33 (CH_3), 22.21 (CH_3), 15.33 (CH_3). HRMS calcd for $C_{19}H_{19}NNaO_2$ $[M + Na]^+$ 316.1308, found 316.1310.

*8,8-Dibenzyl-5-isopropyl-5,6,7,8-tetrahydroindeno[1,2-b]indole-9,10-dione (**4r**).* Orange solid. Yield 35%. Mp 236 °C. IR (ν cm^{-1}): 1707, 1654, 1604, 1527. ^{1}H NMR ($CDCl_3$, 400 MHz) δ: 7.48 (d, 1H, J = 7.1 Hz, Harom), 7.22−7.06 (m, 13H, Harom), 4.45 (m, 1H, $C\underline{H}Me_2$), 3.34 (d, 2H, J = 13.4 Hz, $\underline{CH_2}Ph$), 2.70 (m, 2H, CH_2-6 or CH_2-7), 2.62 (d, 2H, J = 13.6 Hz, $\underline{CH_2}Ph$), 1.93 (m, 2H, CH_2-6 or CH_2-7), 1.53 (d, 6H, J = 7.1 Hz, $CH\underline{Me}_2$). ^{13}C NMR + DEPT ($CDCl_3$, 100 MHz) δ: 194.72 (C=O), 184.28 (C=O), 152.20 (Cquat), 147.40 (Cquat), 139.19 (Cquat), 137.84 (3 Cquat), 135.40 (Cquat), 132.17 (CH), 131.12 (4 CH), 128.29 (CH), 128.07 (4 CH), 126.44 (2 CH), 124.01 (CH), 118.78 (CH), 65.99 (CH_2), 50.66 (2 Cquat), 42.53 (2 CH_2), 29.50 (CH_2), 21.96 (2 CH_3), 15.50 (CH). HRMS calcd for $C_{32}H_{29}NNaO_2$ $[M + Na]^+$ 482.2091, found 482.2106.

X-ray Data. The structure of compounds **4c** has been established by X-ray crystallography (Figure 2). Orange/red single crystal (0.20 × 0.10 × 0.01 mm^3) of **4c** was obtained after 24 h at 21 °C from a closed methanol/chloroform (25/75) solution preliminary heated at 37 °C during 1 h followed by instantaneous cooling at −20 °C during 20 s: orthorhombic, space group $P2_12_12$, a = 15.3192(7) Å, b = 21.1897(10) Å, c = 5.4407(2) Å, α = 90°, β = 90°, γ = 90°, V = 1766.10(13) Å^3, Z = 4, δ(calcd) = 1.284 Mg·m^{-3}, FW = 341.39 for $C_{23}H_{19}NO_2$, F(000) = 720. Crystallographic data were acquired on a Bruker APEX 2 DUO. Full crystallographic results have been deposited at the Cambridge Crystallographic Data Centre (CCDC-867623), U.K.[50] The data were corrected for Lorentz and polarization effects and for empirical absorption correction.[51] The structure was solved by direct methods SHELX 97 and refined using SHELX 97 suite of programs.[52]

Biology and Biochemistry. *Preparation of Recombinant Human CK2 Holoenzyme.* Recombinant human CK2 holoenzyme was prepared according to a modified protocol of Grankowski et al.[53] as described earlier.[54] Human CK2α-subunit (CSNK2A1) and human CK2β-subunit (CSNK2B) were expressed separately using a pT7-7 expression system in *Escherichia coli* BL21(DE3). In detail, freshly transformed starter cultures were grown overnight at 37 °C in LB medium until the stationary phase was reached. Fresh LB medium, inoculated with the separate starter cultures for both subunits, was cultivated until an OD_{500} of 0.6 was reached. Protein expression was induced by the addition of IPTG (1 mM final concentration) and further incubation of the cultures at 30 °C for 5−6 h for the CK2α-subunit and for 3 h for the CK2β-subunit. Bacterial cells were harvested by centrifugation (6000g for 10 min at 4 °C) and disrupted by sonification (3 times 30 s on ice). Cell debris was removed by centrifugation, and the bacterial extracts were combined prior to purification by a three-column procedure. Fractions showing CK2 activity were combined and analyzed by SDS−PAGE and Western blot. The purity of the CK2 holoenzyme was superior to 99%.[15]

Capillary Electrophoresis Based Assay for the Testing of Inhibitors of the Human CK2. Testing of the inhibitors of the human CK2 was performed by the recently established capillary electrophoresis based CK2 activity assay of Gratz et al.[55] An amount of 2 μL of the dissolved inhibitors (stock solution in DMSO) mixed with 78 μL of kinase buffer (50 mM Tris-HCl (pH 7.5), 100 mM NaCl, 10 mM $MgCl_2$, and 1 mM DTT) containing 1 μg of CK2 was preincubated at 37 °C for 10 min. CK2 reaction was initiated by the addition of 120 μL of likewise preincubated assay buffer (25 mM Tris-HCl (pH 8.5), 150 mM NaCl, 5 mM $MgCl_2$, 1 mM DTT, 100 μM ATP, and 0.19 mM of the substrate peptide RRRDDDSDDD). After 15 min the reaction was stopped by the addition of 4 μL of EDTA (0.5 M). The reaction mixture was supplied to a PA800 plus capillary electrophoresis system (Beckman Coulter, Krefeld, Germany) using acetic acid (2 M, adjusted with conc HCl to pH 2.0) as the background electrolyte. The separated substrate and product peptide were detected at 214 nm using a DAD detector. Samples containing pure DMSO served as a control for 0% inhibition, and samples additionally lacking the CK2 holoenzyme served as a control for 100% inhibition. For the initial testing a final inhibitor concentration of 10 μM was applied. Compounds that exhibited at least 50% inhibition at this concentration were subjected to an IC_{50} determination. For this purpose, nine inhibitor concentrations in appropriate intervals ranging from 0.001 to 100 μM were used. IC_{50} values were calculated from the resulting dose−response curves.

Cell Culture and Proliferation. MCF-7 breast cancer cells (kindly provided by the Department of Clinical Radiology of the University Hospital Münster, Germany), were cultured in RPMI 1640 medium—GlutaMax (Life Technologies) and 10% fetal calf serum.[41] They were seeded at a density of 5.0 × 10^4 cells per well into 24-well culture plates. After overnight incubation, seeding medium was removed and replaced with fresh medium containing the inhibitor at 20 or 100 μM. DMSO, at a final concentration of 1%, served as a control. Cells were incubated for 24 or 48 h at 37 °C in a humidified atmosphere (5% CO_2). Cell proliferation was quantified by the EdU-click assay (Baseclick BCK-EdU555-1, Baseclick GmbH, Munich, Germany): the nucleoside analog 5-ethynyl-2′-deoxyuridine is incorporated during active DNA synthesis, and the 5-TAMRA-PEG3-azide fluorophore, used for detection, is coupled by click reaction; afterward, nuclear DNA is stained using the DNA fluorophore **1** (500 μL of 3 μg/mL in methanol) and cells were incubated for 30 min at room temperature in the dark, washed, and finally overlaid with PBS.[42] Cellular fluorescence was monitored with a Keyence BZ-9000 fluorescence microscope (Keyence Corporation, Osaka, Japan) with the "hard-coated" TRITC filter (excitation 543/22 nm; emission 593/40 nm) for TAMRA detection and the "hard coated" DAPI BP filter (excitation 377/50 nm; emission 447/60 nm) for **1** detection. The number of cells exhibiting an active DNA synthesis (staining with fluorophore 5-TAMRA-PEG3-azide) and the total number of cells (Hoechst staining) were counted. The results were expressed as a percent ratio of proliferating cells versus total number of cells.

Compounds. Mitoxantrone was purchased from Sigma-Aldrich (France). All commercial reagents were of the highest available purity grade. The compounds were dissolved in DMSO and then diluted in Dulbecco's modified Eagle medium (DMEM high glucose). The stock solutions were stored at −20 °C and warmed to 25 °C just before use.

Cell Cultures. The human fibroblast HEK293 cell line was transfected with ABCG2 (HEK293-*ABCG2*) as previously described.[44] The cells were maintained in DMEM high glucose supplemented with 10% fetal bovine serum (FBS), 1% penicillin/streptomycin, and 0.75 mg/mL G418 at 37 °C, 5% CO_2 under controlled humidity.

ABCG2-Mediated Mitoxantrone Efflux and Inhibition. As previously,[44] cells were seeded at a density of 1.0×10^5 cells/well into 24-well culture plates. After a 72 h incubation, the cells were exposed to 5 μM mitoxantrone for 30 min at 37 °C, in the presence or absence of each compound, and then washed with phosphate buffer saline (PBS) and trypsinized. The intracellular fluorescence was monitored with a FACS Calibur cytometer (Becton Dickinson) equipped with a 635 nm red laser, using the FL4 channel, and at least 10 000 events were collected. The percentage of inhibition was calculated by using the following equation: % inhibition = $[(C - M)/(C_{ev} - M)] \times 100$, where C is the intracellular fluorescence of resistant cells (HEK293-*ABCG2*) in the presence of compounds and mitoxantrone, M the intracellular fluorescence of resistant cells with only mitoxantrone, and C_{ev} the intracellular fluorescence of control cells (the same HEK293-*ABCG2* cells 100% inhibited with 1 μM Ko143).

Intrinsic Cytotoxicity of the Inhibitory Compounds. Cell viability was evaluated through the MTT colorimetric assay.[56] Wild-type HEK293 cells were seeded at a density of 1×10^4 cells/well, into 96-well culture plates. After overnight incubation, the cells were treated with the compounds (0–250 μM) for 72 h. To assess the viability, the cells were exposed to 0.5 mg/mL of MTT and incubated for 4 h at 37 °C. The culture medium was discarded, and 100 μL of a DMSO/ethanol (1:1) solution was added into each well and mixed by gentle shaking for 10 min. Absorbance was measured at 570 nm using a microplate reader, and the value measured at 690 nm was subtracted. Data are the mean ± SD of at least three independent experiments.

AUTHOR INFORMATION

Corresponding Author

*E-mail: a.dipietro@ibcp.fr. Phone: (+33) 47272 2629. Fax: (+33) 47272 2604.

Author Contributions

×Researchers G.J.G. and Z.B. equally contributed to the experiments.

Author Contributions

○Senior investigators M.L.B. and A.D.P. equally contributed to work supervision.

Notes

The authors declare no competing financial interest.

ACKNOWLEDGMENTS

G.J.G., E.W., and G.V. were recipients of mobility doctoral fellowships from the Brazilian CNPq-CAPES (Science without Borders Program 245762/2012-4) and CAPES (Process Nos. 8792127 and 2303/10-8). N.D.-Y. was a recipient of a postdoctoral fellowship for the Control of Cancer-CNPq (Science without Borders Program). A.N. thanks the Algerian Ministry of Foreign Affairs and the Institut Français d'Algérie for his doctoral fellowship. Financial support was provided by the CNRS and Université Lyon 1 (UMR 5086), the Ligue Nationale Contre le Cancer (Equipe Labellisée Ligue 2014), an international grant from French ANR and Hungarian NIH (Grant 2010-INT-1101-01). The Aquitaine Region is thanked for supporting equipment set up in CESAMO. We thank M. Duong Minh Quang and Thi Huong Nguyen for their assistance during the preparation of compounds **4j**, **4l**, and **4o**, and Dr. Anthony Coleman for improving the English.

ABBREVIATIONS USED

ABC, ATP-binding cassette; ABCG2, breast cancer resistance protein; ARS, aromatic ring system; CK2, casein kinase II; DMA, dimethylacetamide; HBA, hydrogen-bond acceptor; HEK, human embryonic kidney; HP, hydrophobic part; LCIA, lithium cyclohexylisopropylamide; SAR, structure–activity relationship; TETA, *N*,*N*,*N*′,*N*′-tetraethylthionylamide

REFERENCES

(1) Burnett, G.; Kennedy, E. P. The enzymatic phosphorylation of proteins. *J. Biol. Chem.* **1954**, *211*, 969–980.

(2) Giusiano, S.; Cochet, C.; Filhol, O.; Duchemin-Pelletier, E.; Secq, V.; Bonnier, P.; Carcopino, X.; Boubli, L.; Birnbaum, D.; Garcia, S.; Iovanna, J.; Charpin, C. Protein kinase CK2α subunit over-expression correlates with metastatic risk in breast carcinomas: quantitative immunohistochemistry in tissue microarrays. *Eur. J. Cancer* **2011**, *47*, 792–801.

(3) Zhao, T.; Jia, H.; Li, L.; Zhang, G.; Zhao, M.; Cheng, Q.; Zheng, J.; Li, D. Inhibition of CK2 enhances UV-triggered apoptotic cell death in lung cancer cell lines. *Oncol. Rep.* **2013**, *30*, 377–384.

(4) Giroux, V.; Dagorn, J. C.; Iovanna, J. L. A review of kinases implicated in pancreatic cancer. *Pancreatology* **2009**, *9*, 738–754.

(5) Yao, K.; Youn, H.; Gao, X.; Huang, B.; Zhou, F.; Li, B.; Han, H. Casein kinase 2 inhibition attenuates androgen receptor function and cell proliferation in prostate cancer cells. *Prostate* **2012**, *72*, 1423–1430.

(6) Borgo, C.; Cesaro, L.; Salizzato, V.; Ruzzene, M.; Massimino, M. L.; Pinna, L. A.; Donella-Deana, A. Aberrant signalling by protein kinase CK2 in imatinib-resistant chronic myeloid leukaemia cells: biochemical evidence and therapeutic perspectives. *Mol. Oncol.* **2013**, *7*, 1103–1115.

(7) Zheng, Y.; McFarland, B. C.; Drygin, D.; Yu, H.; Bellis, S. L.; Kim, H.; Bredel, M.; Benveniste, E. N. Targeting protein kinase CK2 suppresses prosurvival signaling pathways and growth of glioblastoma. *Clin. Cancer Res.* **2013**, *19*, 6484–6494.

(8) Papinutto, E.; Ranchio, A.; Lolli, G.; Pinna, L. A.; Battistutta, R. Structural and functional analysis of the flexible regions of the catalytic α-subunit of protein kinase CK2. *J. Struct. Biol.* **2012**, *177*, 382–391.

(9) Kinoshita, T.; Nakaniwa, T.; Sekiguchi, Y.; Sogabe, Y.; Sakurai, A.; Nakamura, S.; Nakanishi, I. Crystal structure of human CK2α at 1.06 Å resolution. *J. Synchrotron Radiat.* **2013**, *20*, 974–979.

(10) Cao, J. Y.; Shire, K.; Landry, C.; Gish, G. D.; Pawson, T.; Frappier, L. Identification of a novel protein interaction motif in the regulatory subunit of casein kinase 2. *Mol. Cell. Biol.* **2014**, *34*, 246–258.

(11) Raaf, J.; Guerra, B.; Neundorf, I.; Bopp, B.; Issinger, O. G.; Jose, J.; Pietsch, M.; Niefind, K. First structure of protein kinase CK2 catalytic subunit with an effective CK2β-competitive ligand. *ACS Chem. Biol.* **2013**, *17*, 901–907.

(12) Dobrowolska, G.; Lozeman, F. J.; Li, D.; Krebs, E. G. CK2, a protein kinase of the next millennium. *Mol. Cell. Biochem.* **1999**, *191*, 3–12.

(13) Prudent, R.; Sautel, C. F.; Cochet, C. Structure-based discovery of small molecules targeting different surfaces of protein-kinase CK2. *Biochim. Biophys. Acta* **2010**, *1804*, 493–498.

(14) Hundsdörfer, C.; Hemmerling, H. J.; Götz, C.; Totzke, F.; Bednarski, P.; Le Borgne, M.; Jose, J. Indeno[1,2-*b*]indole derivatives as novel class of potent human protein kinase CK2 inhibitors. *Bioorg. Med. Chem.* **2012**, *20*, 2282–2289.

(15) Guillon, J.; Le Borgne, M.; Rimbault, C.; Moreau, S.; Savrimoutou, S.; Pinaud, N.; Baratin, S.; Marchivie, M.; Roche, S.; Bollacke, A.; Pecci, A.; Alvarez, L.; Desplat, V.; Jose, J. Synthesis and biological evaluation of novel substituted pyrrolo[1,2-*a*]quinoxaline derivatives as inhibitors of the human protein kinase CK2. Eur. *J. Med. Chem.* **2013**, *65*, 205–222.

(16) Hundsdörfer, C.; Hemmerling, H. J.; Hamberger, J.; Le Borgne, M.; Bednarski, P.; Götz, C.; Totzke, F.; Jose, J. Novel indeno[1,2-*b*]indoloquinones as inhibitors of the human protein kinase CK2 with

antiproliferative activity towards a broad panel of cancer cell lines. *Biochem. Biophys. Res. Commun.* **2012**, *424*, 71−75.
(17) Conseil, G.; Perez-Victoria, J. M.; Jault, J.-M.; Gamarro, F.; Goffeau, A.; Hofmann, J.; Di Pietro, A. Protein kinase C effectors bind to multidrug ABC transporters and inhibit their activity. *Biochemistry* **2001**, *40*, 2564−2571.
(18) Erlichman, C.; Boerner, S. A.; Hallgren, C. G.; Spieker, R.; Wang, X. Y.; James, C. D.; Scheffer, G. L.; Maliepaard, M.; Ross, D. D.; Bible, K. C.; Kaufmann, S. H. The HER tyrosine kinase inhibitor CI1033 enhances cytotoxicity of 7-ethyl-10-hydroxycamptothecin and topotecan by inhibiting breast cancer resistance protein-mediated drug efflux. *Cancer Res.* **2001**, *61*, 739−748.
(19) Houghton, P. J.; Germain, G. S.; Harwood, F. C.; Schuetz, J. D.; Stewart, C. F.; Buchdunger, E.; Traxler, P. Imatinib mesylate is a potent inhibitor of the ABCG2 (BCRP) transporter and reverses resistance to topotecan and SN-38 in vitro. *Cancer Res.* **2004**, *64*, 2333−2337.
(20) Yanase, K.; Tsukahara, S.; Asada, S.; Ishikawa, E.; Imai, Y.; Sugimoto, Y. Gefitinib reverses breast cancer resistance protein-mediated drug resistance. *Mol. Cancer Ther.* **2004**, *3*, 1119−1125.
(21) Ozvegy-Laczka, C.; Hegedus, T.; Varady, G.; Ujhelly, O.; Schuetz, J. D.; Varadi, A.; Keri, G.; Orfi, L.; Nemet, K.; Sarkadi, B. High-affinity interaction of tyrosine kinase inhibitors with the ABCG2 multidrug transporter. *Mol. Pharmacol.* **2004**, *65*, 1485−1495.
(22) Dohse, M.; Scharenberg, C.; Shukla, S.; Robey, R. W.; Volkmann, T.; Deeken, J. F.; Brendel, C.; Ambudkar, S. V.; Neubauer, A.; Bates, S. E. Comparison of ATP-binding cassette transporter interactions with the tyrosine kinase inhibitors imatinib, nilotinib, and dasatinib. *Drug Metab. Dispos.* **2010**, *38*, 1371−1380.
(23) Hegedus, C.; Truta-Feles, K.; Antalffy, G.; Varady, G.; Nemet, K.; Ozvegy-Laczka, C.; Keri, G.; Orfi, L.; Szakacs, G.; Varadi, A.; Sarkadi, B. Interaction of the EGFR inhibitors gefitinib, vandetanib, pelitinib and neratinib with the ABCG2 multidrug transporter: implications for the emergence and reversal of cancer drug resistance. *Biochem. Pharmacol.* **2012**, *84*, 260−267.
(24) Lainey, E.; Sébert, M.; Thépot, S.; Scoazec, M.; Bouteloup, C.; Leroy, C.; De Botton, S.; Galluzzi, L.; Fenaux, P.; Kroemer, G. Erlotinib antagonizes ABC transporters in acute myeloid leukemia. *Cell Cycle* **2012**, *11*, 4079−4092.
(25) Mazard, T.; Causse, A.; Simony, J.; Leconet, W.; Vezzio-Vie, N.; Torro, A.; Jarlier, M.; Evrard, A.; Del Rio, M.; Assenat, E.; Martineau, P.; Ychou, M.; Robert, B.; Gongora, C. Sorafenib overcomes irinotecan resistance in colorectal cancer by inhibiting the ABCG2 drug-efflux pump. *Mol. Cancer Ther.* **2013**, *12*, 2121−2134.
(26) Bilbao-Meseguer, I.; Jose, B. S.; Lopez-Gimenez, L. R.; Gil, M. A.; Serrano, L.; Castano, M.; Sautua, S.; Basagoiti, A. D.; Belaustegui, A.; Baza, B.; Baskaran, Z.; Bustinza, A. Drug interactions with sunitinib. *J. Oncol. Pharm. Pract.* Online early access. DOI: 10.1177/1078155213516158. Published Online: January 8, **2014**.
(27) Zhang, H.; Kathawala, R. J.; Wang, Y. J.; Zhang, Y. K.; Patel, A.; Shukla, S.; Robey, R. W.; Talele, T. T.; Ashby, C. R., Jr.; Ambudkar, S. V.; Bates, S. E.; Fu, L. W.; Chen, Z. S. Linsitinib (OSI-906) antagonizes ATP-binding cassette subfamily G member 2 and subfamily C member 10-mediated drug resistance. *Int. J. Biochem. Cell Biol.* **2014**, *51C*, 111−119.
(28) Robey, R. W.; Shukla, S.; Steadman, K.; Obrzut, T.; Finley, E. M.; Ambudkar, S. V.; Bates, S. E. Inhibition of ABCG2-mediated transport by protein kinase inhibitors with a bisindolylmaleimide or indolocarbazole structure. *Mol. Cancer Ther.* **2007**, *6*, 1877−1885.
(29) Sim, H.-M.; Lee, C.-Y.; Ee, P. L. R.; Go, M.-L. Dimethoxyaurones: potent inhibitors of ABCG2 (breast cancer resistance protein). *Eur. J. Pharm. Sci.* **2008**, *35*, 293−306.
(30) Diestra, J. E.; Scheffer, G. L.; Català, I.; Maliepaard, M.; Schellens, J. H.; Scheper, R. J.; Germà-Lluch, J. R.; Izquierdo, M. A. Frequent expression of the multi-drug resistance-associated protein BCRP/MXR/ABCP/ABCG2 in human tumors detected by the BXP-21 monoclonal antibody in paraffin-embedded material. *J. Pathol.* **2002**, *198*, 213−219.
(31) Allen, J. D.; van Loevezijn, A.; Lakhai, J. M.; van der Valk, M.; van Tellingen, O.; Reid, G.; Schellens, J. H. M.; Koomen, G.-J.; Schinkel, A. H. Potent and specific inhibition of the breast cancer resistance protein multidrug transporter in vitro and in mouse intestine by a novel analogue of fumitremorgin C. *Mol. Cancer Ther.* **2002**, *1*, 417−425.
(32) Kühnle, M.; Egger, M.; Müller, C.; Mahringer, A.; Bernhardt, G.; Fricker, G.; König, B.; Buschauer, A. Potent and selective inhibitors of breast cancer resistance protein (ABCG2) derived from the p-glycoprotein (ABCB1) modulator tariquidar. *J. Med. Chem.* **2009**, *52*, 1190−1197.
(33) Hemmerling, H. J.; Reiss, G. Partially saturated indeno[1,2-*b*]indole derivatives via deoxygenation of heterocyclic α-hydroxy-*N*,*O*-hemiaminals. *Synthesis* **2009**, *6*, 985−999.
(34) Richey, H. G.; Farkas, J. Sulfamides and sulfonamides as polar aprotic solvents. *J. Org. Chem.* **1987**, *52*, 479−483.
(35) Lui, W.; Buck, M.; Chen, N.; Shang, M.; Talor, N. J.; Asoud, J.; Wu, X.; Hasinoff, B. B.; Dmitrienko, G. I. Total synthesis of isoprekinamycin: structural evidence for enhanced diazonium ion character and growth inhibitory activity toward cancer cells. *Org. Lett.* **2007**, *l9*, 2915−2918.
(36) Matsuo, K.; Ishida, S. Synthesis of murrayaquinone-A. *Chem. Pharm. Bull.* **1994**, *42*, 1325−1327.
(37) Alchab, F.; Ettouati, L.; Bouaziz, Z.; Bollacke, A.; Delcros, J.-G.; Gertzen, C. G. W.; Gohlke, H.; Pinaud, N.; Marchivie, M.; Guillon, J.; Fenet, B.; Jose, J.; Le Borgne, M. Unpublished results.
(38) Janreddy, D.; Kavala, V.; Bosco, J. W. J.; Kuo, C.-W.; Yao, C.-F. An easy access to carbazolones and 2,3-disubstituted indoles. *Eur. J. Org. Chem.* **2011**, *12*, 2360−2365.
(39) Bill, K.; Black, G. G.; Falshaw, C. P.; Sainsbury, M. The coupling reactions of 3-acylindoles and proof of structure of the palladium(II) acetate mediated cyclisation reaction product of 3-benzoyl-1-methylindole. *Heterocycles* **1983**, *20*, 2433−2436.
(40) Gray, G. K.; McFarland, B. C.; Rowse, A. L.; Gibson, S. A.; Benveniste, E. N. Therapeutic CK2 inhibition attenuates diverse prosurvival signaling cascades and decreases cell viability in human breast cancer cells. *Oncotarget* **2014**, *5*, 6484−6496.
(41) Xue, L.; Chiu, S.; Oleinick, N. L. Staurosporine-induced death of MCF-7 human breast cancer cells: a distinction between caspase-3-dependent steps of apoptosis and the critical lethal lesions. *Exp. Cell Res.* **2003**, *283*, 135−145.
(42) Salic, A.; Mitchinson, T. J. A chemical method for fast and sensitive detection of DNA synthesis in vivo. *Proc. Natl. Acad. Sci. U.S.A.* **2008**, *105*, 2415−2420.
(43) Latt, S. A.; Stetten, G.; Juergens, L. A.; Willard, H. F.; Scher, C. D. Recent developments in the detection of deoxyribonucleic acid synthesis by 33258 Hoescht fluorescence. *J. Histochem. Cytochem.* **1975**, *23*, 493−505.
(44) Winter, E.; Lecerf-Schmidt, F.; Jabor Gozzi, G.; Peres, B.; Lightbody, M.; Gauthier, C.; Ozvegy-Laczka, C.; Szakacs, G.; Sarkadi, B.; Creczynski-Pasa, T.; Boumendjel, A.; Di Pietro, A. Structure−activity relationships of chromone derivatives toward mechanism of interaction with, and inhibition of, breast cancer resistance protein ABCG2. *J. Med. Chem.* **2013**, *56*, 9849−9860.
(45) Ochoa-Puentes, C.; Höcherl, P.; Kühnle, M.; Bauer, S.; Bürger, K.; Bernhardt, G.; Buschauer, A.; König, B. Solid-phase synthesis of tariquidar-related modulators of breast cancer resistance protein (ABCG2). *Bioorg. Med. Chem. Lett.* **2011**, *21*, 3654−3657.
(46) Matsson, P.; Englund, G.; Ahlin, G.; Bergström, C. A. S.; Norinder, U.; Artursson, P. A global drug inhibition pattern for the human ATP-binding cassette transporter breast cancer resistance protein (ABCG2). *J. Pharmacol. Exp. Ther.* **2007**, *323*, 19−30.
(47) Ding, Y.-L.; Shih, Y.-H.; Tsai, F.-H.; Leong, M. K. In silico prediction of inhibition of promiscuous breast cancer resistance protein (BCRP/ABCG2). *PLoS One* **2014**, *9*, e90689.
(48) Stacy, A. E.; Jansson, P. J.; Richardson, D. R. Molecular pharmacology of ABCG2 and its role in chemoresistance. *Mol. Pharmacol.* **2013**, *84*, 655−669.

(49) Lecerf-Schmidt, F.; Peres, B.; Valdameri, G.; Gauthier, C.; Winter, E.; Payen, L.; Di Pietro, A.; Boumendjel, A. ABCG2: recent discovery of potent and highly selective inhibitors. *Future Med. Chem.* **2013**, *5*, 1037−1045.
(50) Supplementary X-ray crystallographic data: Cambridge Crystallographic Data Centre, University Chemical Lab, Lensfield Road, Cambridge, CB2 1EW, U.K.; e-mail, deposit@chemcrys.cam.ac.uk.
(51) Sheldrick, G. M. *SADABS*; University of Göttingen: Göttingen, Germany, 1996.
(52) Sheldrick, G. M. A short history of SHELX. *Acta Crystallogr., Sect. A* **2008**, *64*, 112−122.
(53) Grankowski, N.; Boldyreff, B.; Issinger, O. G. Isolation and characterization of recombinant human casein kinase II subunits α and β from bacteria. *Eur. J. Biochem.* **1991**, *198*, 25−30.
(54) Olgen, S.; Götz, C.; Jose, J. Synthesis and biological evaluation of 3-(substituted-benzylidene)-1,3-dihydroindolin derivatives as human protein kinase CK2 and p60(c-Src) tyrosine kinase inhibitors. *Biol. Pharm. Bull.* **2007**, *30*, 715−718.
(55) Gratz, A.; Götz, C.; Jose, J. A CE-based assay for human protein kinase CK2 activity measurement and inhibitor screening. *Electrophoresis* **2010**, *31*, 634−640.
(56) Mosmann, T. Rapid colorimetric assay for cellular growth and survival. Application to proliferation and cytotoxicity assays. *J. Immunol. Methods* **1983**, *65*, 55−63.